

Double fast algorithm for solving time-space fractional diffusion problems with spectral fractional Laplacian

Yi Yang^a, Jin Huang^{a,*}

^a*School of Mathematical Sciences, University of Electronic Science and Technology of China, Chengdu, 611731, China*

Abstract

This paper presents an efficient and concise double fast algorithm to solve high dimensional time-space fractional diffusion problems with spectral fractional Laplacian. We first establish semi-discrete scheme of time-space fractional diffusion equation, which uses linear finite element or fourth-order compact difference method combining with matrix transfer technique to approximate spectral fractional Laplacian. Then we introduce a fast time-stepping L1 scheme for time discretization. The proposed scheme can exactly evaluate fractional power of matrix and perform matrix-vector multiplication at per time level by using discrete sine transform, which doesn't need to resort to any iteration method and can significantly reduce computation cost and memory requirement. Further, we address stability and convergence analyses of full discrete scheme based on fast time-stepping L1 scheme on graded time mesh. Our analysis shows that the choice of graded mesh factor $\omega = (2 - \alpha)/\alpha$ shall give an optimal temporal convergence $\mathcal{O}(N^{-(2-\alpha)})$ with N denoting the number of time mesh. Finally, ample numerical examples are delivered to illustrate our theoretical analysis and the efficiency of the suggested scheme.

Keywords: Fractional diffusion problem, Spectral fractional Laplacian, Finite element method, Compact difference method, Matrix transfer technique, Convergence analysis

1. Introduction

With the development of science and technology, it has been found that normal diffusion models can not adequately describe many natural phenomena in complex dynamic systems that exhibit power-law decaying behavior [1–5]. Such diffusion usually deviates from the assumption of Brownian motion so that it is called anomalous diffusion. In addition, from a probabilistic point of view, anomalous diffusion commonly follows a relation that the second moment or mean squared displacement of a particle is a nonlinear function of time t , i.e., $\langle |x(t)|^2 \rangle \sim t^\beta$ with $\beta = [0, 1) \cup (1, 2]$, $x(t)$ is the trajectory of a particle or stochastic process [6–8]. Anomalous diffusion phenomena are ubiquitous in natural world, such as diffusive transport of solutes in heterogeneous porous media [9, 10], RNA movement in bacterial cytoplasm [11], animals' food-seeking [12, 13], contaminants in groundwater [14], material with thermal memory [15] and so on.

Of the many possible models of anomalous diffusion, we shall be interested in so-called fractional diffusion, which is a nonlocal process and can be derived to model diffusive transport phenomena of solutes in

*Corresponding author

Email addresses: eyannyee@163.com (Yi Yang), huangjin12345@163.com, huangj@uestc.edu.cn (Jin Huang)

heterogeneous porous media [9, 10]. Specifically, we concentrate on the following nonlocal diffusion model

$$\begin{cases} \partial_t^\alpha u(\mathbf{x}, t) + \kappa_s(-\Delta + \gamma \mathbb{I})^s u(\mathbf{x}, t) = f(\mathbf{x}, t), & \mathbf{x} \in \Omega, \quad 0 < t \leq T, \\ u(\mathbf{x}, 0) = u_0(\mathbf{x}), & \mathbf{x} \in \Omega, \\ u(\mathbf{x}, t) = 0, & \mathbf{x} \in \partial\Omega, \quad 0 < t \leq T, \end{cases} \quad (1)$$

where $0 < s < 1$, $\gamma \geq 0$, $\kappa_s > 0$ is diffusion coefficient, \mathbb{I} denotes identity operator, $\Omega \subset \mathbb{R}^d$ ($d = 1, 2, 3$) is a bounded open domain, and initial value u_0 and source term f are known. Through the framework of a continuous time random walk under the assumption that the mean waiting time has a power-law decaying tail [9, 10], the Caputo derivative of $u(\mathbf{x}, t)$ can be derived as follows:

$$\partial_t^\alpha u(\mathbf{x}, t) = \frac{1}{\Gamma(1-\alpha)} \int_0^t \frac{\partial u(\mathbf{x}, \tau)}{\partial \tau} \frac{d\tau}{(t-\tau)^\alpha}, \quad (2)$$

where $0 < \alpha < 1$, and $\Gamma(\cdot)$ corresponds to Euler's Gamma function.

For the fractional Laplacian $(-\Delta + \gamma \mathbb{I})^s$, a definition of tempered fractional Laplacian was reported in [8] on bounded domain. In this work, we primarily consider the following spectral decomposition form:

$$(-\Delta + \gamma \mathbb{I})^s u(\mathbf{x}, t) = \sum_{j=1}^{\infty} (u, \varphi_j) (\lambda_j + \gamma)^s \varphi_j, \quad (3)$$

where $\{(\lambda_j, \varphi_j)\}_{j=1}^{\infty}$ denote the eigenpairs of classical Laplacian operator $(-\Delta)$ with homogeneous Dirichlet boundary conditions on Ω . When taking $\gamma = 0$ in (3), the fractional Laplacian can represent the infinitesimal generator of a subordinate killed Brownian motion, namely, the process that first kills Brownian motion in Ω and then subordinates it through an s -stable subordinator [3, 6, 7, 16].

Time-space fractional diffusion problems involving spectral fractional Laplacian have attracted considerable attention and been widely studied in pasted decade. But all along, nonlocal nature of time-space fractional differential operators brings scholars great challenges in aspects of analysis and simulation. In [17], a Caffarelli-Silvestre extension turned problem (1) with $\gamma = 0$ into a quasistationary elliptic problem with dynamic boundary condition, which brought one extra dimension and a degenerate weight. The finite element method (FEM) and spectral method based on the Caffarelli-Silvestre extension were introduced in [18–20]. Through Dunford-Taylor integral representation, finite element discretization using sinc quadrature for spectral fractional Laplacian was proposed in [19, 21–23]. Recently, a best uniform rational approximation was found for solving spectral fractional elliptic problems [24–26]. But it is difficult to derive a similar finite element error estimate developed in [24, Theorem 4.1] for time-space fractional diffusion problems. In addition, there were also a family of wildly used numerical methods combining with matrix transfer technique, such as finite difference methods [27–30], FEMs [28, 31–33], and also spectral and spectral element methods [34]. However, the use of matrix transfer technique will encounter a thorny problem that how to treat fractional power of matrix obtained from spatial discretization, which usually leads to high computational cost and thus is rather time-consuming.

To this end, it is necessary to establish concise and implementable solutions for time-space nonlocal model problems. In this paper, we shall be devoted to an efficient implementation of matrix transfer technique. To the best of our current knowledge, some current existing works employing matrix transfer technique [27–29, 32–34] mainly proposed the numerical approximation to fractional power of matrix, and then iteration methods (e.g., Krylov subspace method) for system of equations are necessary. In [30], authors reported a fast second-order central difference scheme and matrix transfer technique for time-space fractional diffusion problem, which can exactly compute the solution of diffusion problem but without theoretical analysis. In addition, we also notice that there is still no literature on finite element analysis for time-space fractional diffusion problem (1) using fast time-stepping L1 scheme on graded temporal mesh.

This paper has two aims. The first goal is to propose an efficient and accurate spatial semi-discrete scheme using linear FEM or fourth-order compact difference method (CDM) and matrix transfer technique for solving problem (1). Since eigen-decomposition of symmetric tri-diagonal Toeplitz matrix coming from finite element or compact difference discretization can be carried out by 1-dimensional discrete sine transform, we extend the technique to deal with spectral fractional Laplacian on d -dimensional Cartesian meshes with the aids of the properties of Kronecker product and generalized multinomial theorem. The method can exactly and fastly evaluate fractional power of matrix and perform matrix-vector multiplication using d -dimensional discrete sine transform at arbitrary time level, and thus enjoys low computational cost and high numerical accuracy. This is significantly different from some existing reports [18, 19, 27–29, 31–33]. The second is to study stability and convergence analyses of full discrete scheme using fast time-stepping L1 scheme on graded temporal mesh. The provided analysis shall illustrate that a choice of graded mesh factor $\omega = (2 - \alpha)/\alpha$ can yield an optimal temporal convergence $\mathcal{O}(N^{-(2-\alpha)})$ in time, where N denotes the number of time intervals.

The main contributions of this paper include the following: (1) efficient finite element or compact difference semi-discretization using matrix transfer technique for time-space fractional diffusion problem is established; (2) stability and error bounds of full discrete scheme based on fast time-stepping L1 method on graded time meshes are discussed; (3) fast and accurate solver for system of equations is designed by discrete sine transform at per time level; (4) commendably concise and implementation-friendly double fast algorithm is proposed.

The remainder of this paper is organized as follows. In Section 2, matrix transfer technique is introduced, and spatial semi-discrete scheme of time-space fractional diffusion problem is derived. In Section 3, full discrete scheme based on a fast time-stepping L1 scheme is developed, and the corresponding stability and error analyses are addressed. Section 4 performs some numerical experiments. A brief summary is made in Section 5.

2. Spatial discretization

Since there are various approximation techniques for spectral fractional Laplacian problems, we shall be committed to study the matrix transform technique [27] in this section.

To this end, we first give a concise introduction of matrix transform technique by using linear FEM or fourth-order CDM to discretize fractional Poisson problem. Then we extend the numerical algorithm to time-space fractional diffusion problem (1), and also derive the corresponding spatial semi-discrete scheme.

2.1. Matrix transform technique

Throughout this paper, let $\Omega = \prod_{k=1}^d (a_k, b_k)$ be a bounded and open domain with $a_k < b_k$, denote by N_k the number of meshgrids, take the spatial mesh size $h_k = \frac{b_k - a_k}{N_k}$, and define a finite dimensional space

$$V_{h_k} = \text{span} \left\{ \phi_0^{(k)}, \phi_1^{(k)}, \dots, \phi_{N_k}^{(k)} \right\}, \quad k = 1, 2, \dots, d,$$

where $\phi_j^{(k)}$ corresponds to piecewise linear basis function for $j = 0, 1, \dots, N_k$. Then the d -dimensional tensorial finite element space V_h^d can be given by

$$V_h^d = V_{h_1} \otimes V_{h_2} \otimes \dots \otimes V_{h_d}, \quad d = 1, 2, 3,$$

where \otimes represents Kronecker product. In addition, we also define an index set

$$\mathcal{T}_d = \{i = (i_1, i_2, \dots, i_d) \mid 1 \leq i_k \leq N_k - 1, \quad k = 1, 2, \dots, d\}.$$

We now consider tensorial linear FEM or fourth-order CDM for fractional Poisson problem

$$\begin{cases} (-\Delta + \gamma \mathbb{I})^s u(\mathbf{x}) = f(\mathbf{x}), & \mathbf{x} \in \Omega, \\ u(\mathbf{x}) = 0, & \mathbf{x} \in \partial\Omega. \end{cases} \quad (4)$$

By matrix transform technique, (4) is formulated as a matrix-vector multiplication form:

$$(M^{-1}S + \gamma I)^s \mathbf{u} = K\mathbf{b}, \quad (5)$$

where I , S , M and \mathbf{b} denote identity matrix, stiffness matrix, mass matrix and right hand side vector, respectively. Here, we let

$$K = K_1 \otimes \cdots \otimes K_{k-1} \otimes K_k \otimes K_{k+1} \otimes \cdots \otimes K_d,$$

with $K_k = I_k$ or M_k^{-1} using finite element discretization, while $K_k = I_k$ by CDM. The explicit I_k and M_k will be defined later. Most notably, we also have

$$S = \sum_{k=1}^d (M_1 \otimes \cdots \otimes M_{k-1} \otimes A_k \otimes M_{k+1} \otimes \cdots \otimes M_d),$$

as well as

$$M = M_1 \otimes \cdots \otimes M_{k-1} \otimes M_k \otimes M_{k+1} \otimes \cdots \otimes M_d, \quad I = I_1 \otimes \cdots \otimes I_{k-1} \otimes I_k \otimes I_{k+1} \otimes \cdots \otimes I_d,$$

where I_k is $(N_k - 1)$ by $(N_k - 1)$ identity matrix,

$$A_k = \begin{pmatrix} a & b & 0 & 0 & \cdots & 0 \\ b & a & b & 0 & \cdots & 0 \\ \vdots & \ddots & \ddots & \ddots & \ddots & \vdots \\ 0 & \cdots & 0 & b & a & b \\ 0 & \cdots & 0 & 0 & b & a \end{pmatrix}, \quad \text{and} \quad M_k = \begin{pmatrix} c & d & 0 & 0 & \cdots & 0 \\ d & c & d & 0 & \cdots & 0 \\ \vdots & \ddots & \ddots & \ddots & \ddots & \vdots \\ 0 & \cdots & 0 & d & c & d \\ 0 & \cdots & 0 & 0 & d & c \end{pmatrix},$$

here, $a = \frac{2}{h_k}$, $b = \frac{-1}{h_k}$, $c = \frac{4h_k}{6}$ and $d = \frac{h_k}{6}$ by FEM, and yet $a = \frac{2}{h_k^2}$, $b = \frac{-1}{h_k^2}$, $c = \frac{10}{12}$ and $d = \frac{1}{12}$ by CDM. It is noteworthy that $(N_k - 1)$ by $(N_k - 1)$ matrices A_k and M_k are symmetric and tri-diagonal, their eigenvalues can be expressed as

$$\lambda_i^{(s_k)} = a - 2|b| \cos\left(\frac{i\pi}{N_k}\right), \quad \text{and} \quad \lambda_i^{(m_k)} = c + 2|d| \cos\left(\frac{i\pi}{N_k}\right),$$

respectively, and the eigenvectors of both of them are $(P_k)_{ij} = \sqrt{\frac{2}{N_k}} \sin\left(\frac{ij\pi}{N_k}\right)$ for $i, j = 1, 2, \dots, N_k - 1$. For more details, see [35–37]. Therefore, the eigen-decompositions of A_k and M_k are separately as follows:

$$A_k = P_k \Lambda_{s_k} P_k^{-1}, \quad \text{and} \quad M_k = P_k \Lambda_{m_k} P_k^{-1}, \quad (6)$$

where the diagonal matrices

$$\Lambda_{s_k} = \text{diag}\left(\lambda_1^{(s_k)}, \lambda_2^{(s_k)}, \dots, \lambda_{N_k-1}^{(s_k)}\right), \quad \text{and} \quad \Lambda_{m_k} = \text{diag}\left(\lambda_1^{(m_k)}, \lambda_2^{(m_k)}, \dots, \lambda_{N_k-1}^{(m_k)}\right).$$

Also, it follows that $P_k = P_k^T = P_k^{-1}$ for $k = 1, 2, \dots, d$.

Below, we shall extend the above numerical algorithm to time-space fractional diffusion problem (1), which will be stated in the next subsection.

2.2. Spatial semi-discretization

In this part, we primarily present a commendably concise and implementation-friendly spatial numerical algorithm for discretizing fractional diffusion problem (1).

Based on the discretization of fractional Poisson problem (4), we immediately have the following matrix-vector multiplication form of (1):

$$(\partial_t^\alpha + \kappa_s(M^{-1}S + \gamma I)^s) \mathbf{u}(t) = K\mathbf{b}(t), \quad (7)$$

where M , S and K are given by (5), and \mathbf{b} denotes a time-dependent right hand side vector function. The next work aims to deal with the fractional power $(M^{-1}S + \gamma I)^s$ appearing in (7).

In terms of the inverse properties of Kronecker products and its matrix multiplication, we have

$$\begin{aligned} M^{-1}S &= \sum_{k=1}^d ((M_1^{-1}M_1) \otimes \cdots \otimes (M_{k-1}^{-1}M_{k-1}) \otimes (M_k^{-1}A_k) \otimes (M_{k+1}^{-1}M_{k+1}) \otimes \cdots \otimes (M_d^{-1}M_d)) \\ &= \sum_{k=1}^d (I_1 \otimes \cdots \otimes I_{k-1} \otimes (M_k^{-1}A_k) \otimes I_{k+1} \otimes \cdots \otimes I_d). \end{aligned}$$

Therefore, we can obtain

$$\begin{aligned} (M^{-1}S + \gamma I) &= \sum_{k=1}^d (I_1 \otimes \cdots \otimes I_{k-1} \otimes (M_k^{-1}A_k) \otimes I_{k+1} \otimes \cdots \otimes I_d \\ &\quad + \frac{\gamma}{d} I_1 \otimes \cdots \otimes I_{k-1} \otimes I_k \otimes I_{k+1} \otimes \cdots \otimes I_d) \\ &= \sum_{k=1}^d \left(I_1 \otimes \cdots \otimes I_{k-1} \otimes (M_k^{-1}A_k + \frac{\gamma}{d} I_k) \otimes I_{k+1} \otimes \cdots \otimes I_d \right). \end{aligned} \quad (8)$$

Moreover, leveraging eigen-decomposition (6), we derive

$$T_k := (M_k^{-1}A_k + \frac{\gamma}{d} I_k) = P_k \Lambda_k P_k^{-1}, \quad (9)$$

where $\Lambda_k := \text{diag}(\lambda_1^{(k)}, \lambda_2^{(k)}, \dots, \lambda_{N_k-1}^{(k)})$ with $\lambda_i^{(k)} = \left(\frac{\lambda_i^{(s_k)}}{\lambda_i^{(m_k)}} + \frac{\gamma}{d} \right)$ for $i = 1, 2, \dots, N_k - 1$.

Combining (8) and (9), and using generalized multinomial theorem (see [38–40]) yield

$$\begin{aligned} (M^{-1}S + \gamma I)^s &= \left(\sum_{k=1}^d (I_1 \otimes \cdots \otimes I_{k-1} \otimes T_k \otimes I_{k+1} \otimes \cdots \otimes I_d) \right)^s \\ &= \sum_{n_{d-1}=0}^{\infty} \sum_{n_{d-2}=0}^{n_{d-1}} \cdots \sum_{n_1=0}^{n_2} \binom{s}{n_{d-1}} \binom{n_{d-1}}{n_{d-2}} \cdots \binom{n_2}{n_1} (I_1 \otimes \cdots \otimes I_{d-1} \otimes T_d)^{s-n_{d-1}} \\ &\quad \times (I_1 \otimes \cdots \otimes I_{d-2} \otimes T_{d-1} \otimes I_d)^{n_{d-1}-n_{d-2}} \cdots (T_1 \otimes I_2 \otimes \cdots \otimes I_d)^{n_1} \\ &= \sum_{n_{d-1}=0}^{\infty} \sum_{n_{d-2}=0}^{\infty} \cdots \sum_{n_1=0}^{\infty} \binom{s}{n_1, n_2, \dots, n_{d-1}} (T_1 \otimes I_2 \otimes \cdots \otimes I_d)^{n_1} \cdots \\ &\quad \times (I_1 \otimes \cdots \otimes I_{d-2} \otimes T_{d-1} \otimes I_d)^{n_{d-1}} (I_1 \otimes \cdots \otimes I_{d-1} \otimes T_d)^{s-n_1-\cdots-n_{d-1}}, \end{aligned} \quad (10)$$

where the generalized multinomial coefficient

$$\binom{s}{n_1, n_2, \dots, n_{d-1}} := \binom{s}{n_1 + n_2 + \cdots + n_{d-1}} \binom{n_1 + n_2 + \cdots + n_{d-1}}{n_1 + n_2 + \cdots + n_{d-2}} \cdots \binom{n_1 + n_2}{n_1}.$$

In what follows, the treatment means of (10) will be coincidence with [30]. So we directly have

$$(M^{-1}S + \gamma I)^s \mathbf{u}(t) = P_1 \otimes_1 \cdots \otimes_{d-1} P_d \otimes_d (H_d \odot (P_1^{-1} \otimes_1 \cdots \otimes_{d-1} P_d^{-1} \otimes_d U(t))), \quad (11)$$

where H_d is a d -dimensional array denoted by

$$(H_d)_{i_1, i_2, \dots, i_d} = \left(\sum_{k=1}^d \lambda_{i_k}^{(k)} \right)^s, \quad (i_1, i_2, \dots, i_d) \in \mathcal{T}_d. \quad (12)$$

Further, \odot represents Hadamard array product, $U(t) = \{\mathbf{u}_i(t)\}_{(N_1-1) \times \dots \times (N_d-1)}$ is a d -dimensional array for $i \in \mathcal{T}_d$, and the notation \otimes_k is defined by

$$(W \otimes_k R)_{i_1, i_2, \dots, i_d} := \sum_{j=1}^{N_k-1} W_{i_k, j} R_{i_1, \dots, i_{k-1}, j, i_{k+1}, \dots, i_d},$$

where W corresponds to an $(N_k - 1)$ by $(N_k - 1)$ matrix, and R denotes a d -dimensional array.

Next, we give an explicit computation of right hand side vector. Analogous to (11), we shall have

$$\begin{aligned} K \mathbf{b}(t) &= (K_1 \otimes \cdots \otimes K_{k-1} \otimes K_k \otimes K_{k+1} \otimes \cdots \otimes K_d) \mathbf{b}(t) \\ &= P_1 \otimes_1 \cdots \otimes_{d-1} P_d \otimes_d (V_d \odot (P_1^{-1} \otimes_1 \cdots \otimes_{d-1} P_d^{-1} \otimes_d F(t))), \end{aligned} \quad (13)$$

where V_d is a d -dimensional array with entry

$$(V_d)_{i_1, i_2, \dots, i_d} = \prod_{k=1}^d \bar{\lambda}_{i_k}^{(k)}, \quad (i_1, i_2, \dots, i_d) \in \mathcal{T}_d, \quad (14)$$

where $\bar{\lambda}_{i_k}^{(k)}$ means the i_k 'th eigenvalue of K_k , and $F(t) = \{\mathbf{b}_{i_1, i_2, \dots, i_d}(t)\}_{(N_1-1) \times \dots \times (N_d-1)}$ is a d -dimensional array given by

$$\mathbf{b}_{i_1, i_2, \dots, i_d}(t) = f(x_{1_{i_1}}, x_{2_{i_2}}, \dots, x_{d_{i_d}}, t), \quad \text{or} \quad \mathbf{b}_{i_1, i_2, \dots, i_d}(t) = \left(f(\cdot, t), \prod_{k=1}^d \phi_{i_k}^{(k)}(\cdot) \right), \quad (15)$$

where (\cdot, \cdot) denotes L^2 inner product which will be defined later. It should be pointed out by (15) that the former is obtained using finite element discretization with assumption $f(t) \approx f_h(t) \in V_h^d$ or employing CDM directly, at this time one shall choose $K = I$; however, the latter will appear in finite element case, then we have to take $K = M^{-1}$.

In addition, it follows from [30, 41, 42] that

$$P_1 \otimes_1 \cdots \otimes_{d-1} P_d \otimes_d R = \mathcal{D}_d(R), \quad \text{and} \quad P_1^{-1} \otimes_1 \cdots \otimes_{d-1} P_d^{-1} \otimes_d R = \mathcal{D}_d^{-1}(R), \quad (16)$$

where \mathcal{D}_d and \mathcal{D}_d^{-1} represent d -dimensional discrete sine transform and its inverse transform, respectively, and R is a d -dimensional array.

Hence, using (7), (11), (13) and (16), the semi-discrete scheme of problem (1) can be written as

$$\partial_t^\alpha U(t) + \mathcal{D}_d(\kappa_s H_d \odot \mathcal{D}_d^{-1}(U(t))) = \mathcal{D}_d(V_d \odot \mathcal{D}_d^{-1}(F(t))), \quad t \in (0, T]. \quad (17)$$

Remark 1. For the fractional Poisson problem (4), its numerical solution becomes

$$U = \mathcal{D}_d(L_d \odot (V_d \odot \mathcal{D}_d^{-1}(F))),$$

where $F = \{\mathbf{b}_i\}_{(N_1-1) \times \dots \times (N_d-1)}$ is a d -dimensional array for $i \in \mathcal{T}_d$, and L_d is defined by

$$(L_d)_{i_1, i_2, \dots, i_d} = 1/(\kappa_s H_d)_{i_1, i_2, \dots, i_d}, \quad (i_1, i_2, \dots, i_d) \in \mathcal{T}_d.$$

In particular, if taking $f(\mathbf{x}) \approx f_h(\mathbf{x}) \in V_h^d$, then

$$U = \mathcal{D}_d (L_d \odot \mathcal{D}_d^{-1}(F)),$$

where $F = \left\{ f(x_{1_{i_1}}, x_{2_{i_2}}, \dots, x_{d_{i_d}}) \right\}_{(N_1-1) \times \dots \times (N_d-1)}$ denotes a d -dimensional array.

From Remark 1, it should be mentioned that the fast algorithm can reduce the computational cost from $\mathcal{O}(\mathcal{M}^{d+1})$ by a direct matrix-vector multiplication to $\mathcal{O}(\mathcal{M}^d \log_2 \mathcal{M})$ with $\mathcal{M} = \max_{1 \leq k \leq d} N_k$.

Remark 2. If $M = K = I$ in the fourth-order CDM, then (7) or (17) reduces to the second-order central finite difference semi-discrete scheme [30] for (1) in space.

For the present algorithm above, due to the uses of discrete sine transform and its inverse transform, we can exactly evaluate fractional power of matrix (10) and perform the matrix-vector multiplication in (17), which is different from some existing techniques [18, 19, 27–29, 31–33] with high computational cost and low numerical accuracy.

Hereto, we have completed the introduction on the spatial numerical algorithm, which is both concise and implementable. In the next section, we will address the implementation and convergence analysis of full discrete scheme which is based on a fast time-stepping L1 method [43–46] in time.

3. Implementation and analysis of full discrete scheme

Though a fast Fourier algorithm has been presented in space, it is still difficult for us to numerically simulate the high dimensional time-space fractional diffusion problem (1) in temporal direction. Hence, it is critical to choose a discrete technique with low memory and computational cost for problem (1) involving time fractional Caputo derivative (2).

In this part, we first introduce a fast time-stepping L1 scheme for time discretization, and induce the full discrete scheme of (1). Further, we shall give convergence analysis of full discrete scheme.

3.1. Fast time-stepping method

Let N be the number of temporal meshes, and \mathcal{I}^1 the piecewise linear Lagrange interpolation operator. Given temporal graded mesh $t_n = T(n/N)^\omega$ with $\omega \geq 1$ and $n = 1, 2, \dots, N$, we take $t = t_n$ such that

$$\partial_t^\alpha \mathbf{u}(t_n) = \frac{1}{\Gamma(1-\alpha)} \int_0^{t_n} \frac{d\mathbf{u}(\zeta)}{d\zeta} (t_n - \zeta)^{-\alpha} d\zeta, \quad n = 1, 2, \dots, N.$$

Interpolating linearly $\mathbf{u}(\zeta)$ with respect to variable ζ on $[t_{k-1}, t_k]$ for $k = 1, 2, \dots, n$, and using the integration by parts on $[0, t_{n-1}]$, we have

$$\begin{aligned} \partial_t^\alpha \mathbf{u}(t_n) &\approx \frac{1}{\Gamma(1-\alpha)} \int_{t_{n-1}}^{t_n} \frac{d\mathcal{I}^1 \mathbf{u}(\zeta)}{d\zeta} (t_n - \zeta)^{-\alpha} d\zeta + \frac{1}{\Gamma(1-\alpha)} \int_0^{t_{n-1}} \frac{d\mathcal{I}^1 \mathbf{u}(\zeta)}{d\zeta} (t_n - \zeta)^{-\alpha} d\zeta \\ &= \frac{\mathbf{u}(t_n) - \alpha \mathbf{u}(t_{n-1}) - (1-\alpha) \Delta t_n^\alpha t_n^{-\alpha} \mathbf{u}(t_0)}{\tau_n} + \frac{1}{\Gamma(-\alpha)} \int_0^{t_{n-1}} \frac{\mathcal{I}^1 \mathbf{u}(\zeta)}{(t_n - \zeta)^{1+\alpha}} d\zeta \\ &=: L^\alpha \mathbf{u}(t_n) + H^\alpha \mathbf{u}(t_n), \end{aligned} \tag{18}$$

where $\tau_n = \Delta t_n^\alpha \Gamma(2 - \alpha)$, $L^\alpha \mathbf{u}(t_n)$ and $H^\alpha \mathbf{u}(t_n)$ are called local part and history part, respectively.

In order to develop fast time-stepping L1 method, we now introduce a sum of exponentials [43–46] to approximate the kernel $(t_n - \zeta)^{-1-\alpha}$. In this work, we primarily consider the approximation which is based on the trapezoidal rule on a real line. Namely, using the definition of Euler integral representation of Gamma function, a change of variable $s = e^y$ and $\Gamma(1 - \alpha)\Gamma(\alpha) = \frac{\pi}{\sin(\pi\alpha)}$ gives

$$\frac{t^{-\alpha-1}}{\Gamma(-\alpha)} = \frac{1}{\Gamma(-\alpha)\Gamma(\alpha+1)} \int_0^\infty s^\alpha e^{-st} ds = \int_{-\infty}^\infty g(y, t, \alpha) dy, \quad (19)$$

where $g(y, t, \alpha) = -\frac{\sin(\pi\alpha)}{\pi} e^{(\alpha+1)y} e^{-e^y t}$ which decays exponentially as $|y| \rightarrow \infty$. Therefore, we can use the exponentially convergent trapezoidal rule [47] to approximate the integral

$$\int_{-\infty}^\infty g(y, t, \alpha) dy \approx \Delta y \sum_{j=-\infty}^\infty g(j\Delta y, t, \alpha) = \sum_{j=1}^Q w_j e^{\xi_j t} + O(\epsilon t^{-\alpha-1}), \quad t \in [t_1, T], \quad (20)$$

where $Q > 1$ is a positive integer, $w_j = -\frac{\sin(\alpha\pi)}{\pi} \Delta y e^{(1+\alpha)y_j}$, $\xi_j = -e^{y_j}$, $y_j = y_{\min} + (j-1)\Delta y$, $\Delta y = \frac{y_{\max} - y_{\min}}{Q-1}$, and $\epsilon > 0$ is a given precision satisfying

$$\left| \int_{-\infty}^a g(y, t, \alpha) dy \right| + \left| \int_b^\infty g(y, t, \alpha) dy \right| \leq 2\epsilon t^{-1-\alpha}, \quad a < 0 < b. \quad (21)$$

The use of (21) determines $y_{\min} = (1 + \alpha)^{-1} \ln(\epsilon) - \ln(T) \geq a$ and $y_{\max} = \ln\left(\frac{-\ln(\epsilon) + (1+\alpha)\ln(t_1)}{0.5t_1}\right) \leq b$. For some detailed derivations, we refer reader to [48, Appendix C].

Indeed, the above inequality (21) is obvious. A change of variable leads to

$$\left| \int_b^\infty g(y, t, \alpha) dy \right| \leq t^{-\alpha-1} \Gamma(\alpha+1, te^b), \quad \text{and} \quad \left| \int_{-\infty}^a g(y, t, \alpha) dy \right| \leq t^{-\alpha-1} \gamma(\alpha+1, te^a),$$

where $\Gamma(\cdot, \cdot)$ and $\gamma(\cdot, \cdot)$ denote upper and lower incomplete Gamma functions, respectively. For larger b ($b > 0$) and smaller a ($a < 0$), $\Gamma(\alpha+1, te^b)$ and $\gamma(\alpha+1, te^a)$ decay exponentially to 0 so that it is feasible to take ϵ to be as follows:

$$\epsilon = \max \{ \Gamma(\alpha+1, te^b), \gamma(\alpha+1, te^a) \}. \quad (22)$$

Thus we obtain (21).

Hence, from (19) and (20), we immediately have

$$H^\alpha \mathbf{u}(t_n) = \sum_{j=1}^Q w_j e^{\xi_j \Delta t_n} Y_j(t_{n-1}), \quad (23)$$

where $Y_j(t) = \int_0^t e^{\xi_j(t-\zeta)} \mathcal{I}^1 \mathbf{u}(\zeta) d\zeta$ satisfies

$$(Y_j)'(t) = \xi_j Y_j(t) + \mathcal{I}^1 \mathbf{u}(t) \quad \text{with} \quad Y_j(0) = 0,$$

which can be exactly solved by

$$Y_j(t_i) = \kappa_1 Y_j(t_{i-1}) + \kappa_2 \mathbf{u}(t_{i-1}) + \kappa_3 \mathbf{u}(t_i) \quad \text{with} \quad Y_j(t_0) = 0, \quad i \geq 1,$$

where $\kappa_1 = e^z$, $\kappa_2 = \frac{1}{\xi_j} (e^z - 1 - \frac{e^z - z - 1}{z})$, $\kappa_3 = \frac{1}{\xi_j} \frac{e^z - z - 1}{z}$ and $z = \xi_j \Delta t_i$.

Combining (18) and (23), $\partial_t^\alpha \mathbf{u}(t)$ at $t = t_n$ can be approximated by

$$\partial_t^\alpha \mathbf{u}(t_n) = \bar{\partial}_t^\alpha \mathbf{u}(t_n) + r^n, \quad (24)$$

where r^n denotes truncation error, and the discrete differential operator $\bar{\partial}_t^\alpha$ is defined by

$$\bar{\partial}_t^\alpha \mathbf{u}(t_n) := \frac{\mathbf{u}(t_n) - \alpha \mathbf{u}(t_{n-1}) - (1 - \alpha) \Delta t_n^\alpha t_n^{-\alpha} \mathbf{u}(t_0)}{\tau_n} + \sum_{j=1}^Q w_j e^{\xi_j \Delta t_n} Y_j(t_{n-1}), \quad n = 1, 2, \dots, N,$$

where the above sum term will vanish for $n = 1$.

From (7) and (24), we shall have

$$(1 + \tau_n \kappa_s (M^{-1} S + \gamma I)^s) \mathbf{u}(t_n) = \mathbf{g}(t_n) + \tau_n K \mathbf{b}(t_n) - r^n, \quad (25)$$

where $\mathbf{g}(t_n)$ is defined by

$$\mathbf{g}(t_n) := \alpha \mathbf{u}(t_{n-1}) + (1 - \alpha) \Delta t_n^\alpha t_n^{-\alpha} \mathbf{u}(t_0) - \tau_n \sum_{j=1}^Q w_j e^{\xi_j \Delta t_n} Y_j(t_{n-1}).$$

Now let \mathbf{u}^n be an approximation to $\mathbf{u}(t_n)$, and \mathbf{g}_i^n the approximation to $\mathbf{g}_i(t_n)$ for $i \in \mathcal{T}_d$. From (11), (13), (16) and (25), we obtain the following fully discrete scheme

$$\mathcal{D}_d((E_d + \tau_n \kappa_s H_d) \odot \mathcal{D}_d^{-1}(U^n)) = G_d^n + \tau_n \mathcal{D}_d(V_d \odot \mathcal{D}_d^{-1}(F^n)), \quad n = 1, 2, \dots, N, \quad (26)$$

where E_d is a d -dimensional array with entry $(E_d)_i = 1$ for $i \in \mathcal{T}_d$, H_d and V_d are given in (12) and (14), respectively. In addition, $U^n = \{\mathbf{u}_i^n\}_{(N_1-1) \times \dots \times (N_d-1)}$, $F^n = \{\mathbf{b}_i(t_n)\}_{(N_1-1) \times \dots \times (N_d-1)}$ and $G_d^n = \{\mathbf{g}_i^n\}_{(N_1-1) \times \dots \times (N_d-1)}$ are three d -dimensional arrays for $i \in \mathcal{T}_d$.

By taking inverse and forward discrete sine transform on both sides of (26) successively, we then have

$$U^n = \mathcal{D}_d(L_d \odot (G_d^n + \tau_n (V_d \odot \mathcal{D}_d^{-1}(F^n))))), \quad n = 1, 2, \dots, N, \quad (27)$$

where L_d denotes a d -dimensional array defined by

$$(L_d)_{i_1, i_2, \dots, i_d} := \frac{1}{1 + \tau_n \kappa_s (H_d)_{i_1, i_2, \dots, i_d}}, \quad (i_1, i_2, \dots, i_d) \in \mathcal{T}_d.$$

Numerical solutions obtained by direct L1 scheme possess heavy history dependence, namely, the solutions of the current time step t_n always depends on the solutions of all previous time steps t_k for $k = 0, 1, \dots, n-1$. However, the fast scheme (27) shows that the solution of the current time step t_n indirectly depends on the solutions of time steps t_{n-1} , t_{n-2} and t_0 . For overall computational complexity, the present double fast algorithm reduces computational cost from $\mathcal{O}(N^2 \mathcal{M}^{d+1})$ to $\mathcal{O}(NQ \mathcal{M}^d \log_2 \mathcal{M})$, where $Q \ll N$.

Remark 3. As $\alpha \rightarrow 1^-$, the numerical solution in (27) reduces to

$$U^n = \mathcal{D}_d(L_d \odot (\mathcal{D}_d^{-1}(U^{n-1}) + \tau_n (V_d \odot \mathcal{D}_d^{-1}(F^n))))), \quad n = 1, 2, \dots, N,$$

where $\tau_n = \Delta t_n$, i.e., a standard first-order backward difference scheme is used for space fractional diffusion problem.

3.2. Convergence analysis

In this subsection, we are devoted to studying stability and convergence analysis of full discrete scheme (26) based on fast time-stepping L1 scheme. To this end, we first recall some basic function spaces, and then introduce Mittag-Leffler function and standard projection estimate. Afterwards, we also give several lemmata which play important roles in the subsequent analysis.

Now, it remains to recall some basic function spaces. Let $H^l(\Omega)$ and $H_0^l(\Omega)$ denote Sobolev spaces with $l \geq -1$, and $\|\cdot\|_l$ and $(\cdot, \cdot)_l$ represent the corresponding H^l -norm and inner product, respectively. If $l = 0$, we shall omit subscript l . For $s \geq -1$, $\dot{H}^s(\Omega) \subset H^{-1}(\Omega)$ denotes a Hilbert space equipped with norm

$$\|v\|_{\dot{H}^s(\Omega)} = \sqrt{\sum_{j=1}^{\infty} (\lambda_j + \gamma)^s (v, \varphi_j)^2}, \quad \gamma \geq 0.$$

Given a Banach space X and arbitrary $p \geq 1$, we can define

$$L^p(0, T; X) = \{v(t) \in X \text{ for a.e. } t \in (0, T) \text{ and } \|v\|_{L^p(0, T; X)} < \infty\},$$

and its norm $\|\cdot\|_{L^p(0, T; X)}$ is induced by

$$\|v\|_{L^p(0, T; X)} = \begin{cases} \left(\int_0^T \|v(t)\|_X^p dt \right)^{1/p}, & p \in [1, \infty), \\ \text{ess sup}_{t \in (0, T)} \|v(t)\|_X, & p = \infty. \end{cases}$$

To derive the mild solution of (1), it is essential to introduce Mittag-Leffler function [49, formula 1.56]

$$E_{\alpha, \beta}(z) = \sum_{k=0}^{\infty} \frac{z^k}{\Gamma(k\alpha + \beta)}, \quad z \in \mathbb{C},$$

where $\beta \in \mathbb{R}$ and $0 < \alpha < 1$. Here, we also give the Fourier expansions of the data u_0 , f and u . Namely, let $u(t) := \sum_{j=1}^{\infty} (u(\cdot, t), \varphi_j) \varphi_j$, $f(t) := \sum_{j=1}^{\infty} (f(\cdot, t), \varphi_j) \varphi_j$ and $u_0 := \sum_{j=1}^{\infty} (u_0(\cdot), \varphi_j) \varphi_j$.

Hence, using method of separation of variables and resorting to the Mittag-Leffler function $E_{\alpha, \beta}$, the mild solution u of problem (1) can be represented as

$$u(t) = E(t)u_0 + \int_0^t \bar{E}(t - \tau) f(\tau) d\tau, \quad (28)$$

where the solution operator

$$E(t)u_0 = \sum_{j=1}^{\infty} E_{\alpha, 1}(-\kappa_s(\lambda_j + \gamma)^s t^\alpha) (u_0, \varphi_j) \varphi_j,$$

and the solution operator \bar{E} for $\chi \in L^2(\Omega)$ is defined by

$$\bar{E}(t)\chi = \sum_{j=1}^{\infty} t^{\alpha-1} E_{\alpha, \alpha}(-\kappa_s(\lambda_j + \gamma)^s t^\alpha) (\chi, \varphi_j) \varphi_j.$$

Before studying the error analysis of full discrete scheme, we also need to give two important properties on the function $E_{\alpha, \beta}$, which can be seen in [49, Theorem 1.6, formula 1.99].

Lemma 3.1. *Let $0 < \alpha < 1$, $\beta \in \mathbb{R}$, and $\frac{\alpha\pi}{2} < \mu < \pi\alpha$. Then there exists constant $C = C(\alpha, \beta, \mu) > 0$ such that*

$$E_{\alpha, \beta}(z) \leq \frac{C}{1 + |z|}, \quad \mu \leq |\arg(z)| \leq \pi, \quad z \in \mathbb{C}.$$

Lemma 3.2. Suppose that $\eta > 0$, $\mu > 0$, and $\alpha > 0$. Then one has

$$\int_0^\eta \tau^{\alpha-1} E_{\alpha,\alpha}(-\mu\tau^\alpha) d\tau = -\frac{1}{\mu} \int_0^\eta \frac{d}{d\tau} E_{\alpha,1}(-\mu\tau^\alpha) d\tau = \frac{1}{\mu} (1 - E_{\alpha,1}(-\mu\eta^\alpha)).$$

It is easy to check that $(-\Delta + \gamma\mathbb{I})$ is a positive self-adjoint operator. Then for all $u \in \dot{H}^{2s}(\Omega)$ and v belonging to a Hilbert space, using Balakrishnan's integral representation, we denote

$$\mathcal{A}(u, v) := ((-\Delta + \gamma\mathbb{I})^s u, v) = \frac{\sin(\pi s)}{\pi} \int_0^\infty (z^{s-1} (-\Delta + \gamma\mathbb{I})(z\mathbb{I} + (-\Delta + \gamma\mathbb{I}))^{-1} u, v) dz. \quad (29)$$

From [32], introducing a elliptic projection $P_h : H_0^{r+1}(\Omega) \rightarrow V_h^d$ such that for $u \in H_0^{r+1}(\Omega)$, we have

$$\mathcal{A}(P_h u - u, v_h) = 0, \quad \forall v_h \in V_h^d.$$

Hence, the following projection estimate holds

$$\|v - P_h v\| \leq Ch^{r+1} \|v\|_{r+1}, \quad \forall v \in H_0^{r+1}(\Omega), \quad (30)$$

where h denotes maximum of h_j for $j = 1, 2, \dots, d$. Besides, we also define a linear bijection $\pi_h : V_h^d \rightarrow \mathbb{R}^m$ such that $\pi_h(u_h) = \mathbf{u}$, where \mathbf{u} means solution vector, and $m = \prod_{j=1}^d (N_j - 1)$ corresponds to the number of degrees of freedom.

Though the proposed fast finite element scheme is based on the linear interpolation, the following discussions can also be extended to high order polynomial interpolation. Next, we primarily study the finite element error analysis of full discrete scheme, but it is also valid when $r \in \mathbb{N}^+$ and $r \geq 1$.

Lemma 3.3. Let $(-\Delta_h + \gamma\mathbb{I})^s = \pi_h^{-1}(M^{-1}S + \gamma I)^s \pi_h$ denote discrete spectral fractional Laplacian operator. Then the following estimation holds:

$$|\mathcal{A}(\varphi_j, v_h) - \mathcal{A}_h(P_h \varphi_j, v_h)| \leq Ch^{r+1} (\lambda_j + \gamma)^s \|\varphi_j\|_{r+1} \|v_h\|, \quad \forall v_h \in V_h^d,$$

where C is a positive constant independent of h , and $\mathcal{A}_h(\cdot, \cdot)$ is defined by

$$\mathcal{A}_h(u_h, v_h) := ((-\Delta_h + \gamma\mathbb{I})^s u_h, v_h), \quad u_h, v_h \in V_h^d.$$

It suffices to prove Lemma 3.3 by (29), (30) and a similar technique developed in [32, Proposition 1].

Lemma 3.4. Let $\{\rho(t_k)\}_{k=0}^n$ denote a series for $n = 1, 2, \dots, N$, and define

$$\sum_{k=0}^n b_k^n \rho(t_k) := \frac{\rho(t_n)}{\tau_n} - \frac{\alpha \rho(t_{n-1})}{\tau_n} - \frac{(1-\alpha)}{\tau_n} \left(\frac{\Delta t_n}{t_n} \right)^\alpha \rho(t_0) + \sum_{j=1}^Q w_j e^{\xi_j \Delta t_n} Y_j(t_{n-1}).$$

Then we have $b_n^n = \frac{1}{\tau_n}$. In addition, if $n = 1$, it follows that

$$b_0^1 = -\frac{\alpha}{\tau_1} - \frac{(1-\alpha)}{\tau_1} \left(\frac{\Delta t_1}{t_1} \right)^\alpha = -\frac{1}{\tau_1}.$$

If $n = 2$, there holds

$$b_0^2 = \sum_{j=1}^Q w_j e^{\xi_j \Delta t_2} k_2 - \frac{(1-\alpha)}{\tau_2} \left(\frac{\Delta t_2}{t_2} \right)^\alpha, \quad b_1^2 = \sum_{j=1}^Q w_j e^{\xi_j \Delta t_2} k_3 - \frac{\alpha}{\tau_2}.$$

If $n \geq 3$, one has

$$\begin{aligned} b_0^n &= \sum_{j=1}^Q w_j e^{\xi_j \Delta t_n} k_1^{n-2} k_2 - \frac{(1-\alpha)}{\tau_n} \left(\frac{\Delta t_n}{t_n} \right)^\alpha, \quad b_{n-1}^n = \sum_{j=1}^Q w_j e^{\xi_j \Delta t_n} k_3 - \frac{\alpha}{\tau_n}, \\ b_i^n &= \sum_{j=1}^Q w_j e^{\xi_j \Delta t_n} (k_1 k_3 + k_2) k_1^{n-2-i}, \quad i = 1, 2, \dots, n-2. \end{aligned}$$

To be more convenient for our analysis, we shall denote

$$\bar{c}_{n,1} := -b_0^n; \quad \bar{c}_{n,n} := b_n^n; \quad \bar{c}_{n,k} := \bar{c}_{n,k-1} - b_{k-1}^n, \quad k = 2, 3, \dots, n. \quad (31)$$

Then it can be noted that $\{\bar{c}_{n,k}\}_{k=1}^n$ enjoy explicit representation using $\{b_k^n\}_{k=1}^n$ in Lemma 3.4. In addition, it also follows that

$$\bar{c}_{n,k} \geq \bar{c}_{n,k-1} \geq \dots \geq \bar{c}_{n,1} \geq \frac{t_n^{-\alpha}}{\Gamma(1-\alpha)} > 0, \quad k = 1, 2, \dots, n.$$

To prove the above inequality, it just needs to show that $b_{k-1}^n \leq 0$ for $k = 1, 2, \dots, n$. According to monotonicities of k_1 , k_2 and k_3 , we have $k_1 \geq 0$, $k_2 \geq 0$, $k_3 \geq 0$, $k_1^{n-2} k_2 \geq 0$ and $(k_1 k_3 + k_2) k_1^{n-2-i} \geq 0$ in Lemma 3.4. Then combining negativity of $\{w_j\}_{j=1}^Q$ in Lemma 3.4 and (20), we can obtain the desired result.

Now, we present the full discrete scheme based on fast time-stepping L1 scheme in time and conforming FEM in space. Find $u_h^n \in V_h^d$ such that

$$(\bar{\partial}_t^\alpha u_h^n, v_h) + \kappa_s \mathcal{A}_h(u_h^n, v_h) = (f, v_h), \quad \forall v_h \in V_h^d, \quad (32)$$

where $\mathcal{A}_h(\cdot, \cdot)$ is given in Lemma 3.3, and discrete differential operator $\bar{\partial}_t^\alpha$ in (24) is rewritten as

$$\bar{\partial}_t^\alpha u_h^n = \sum_{k=1}^n \bar{c}_{n,k} (u_h^k - u_h^{k-1}), \quad n = 1, 2, \dots, N. \quad (33)$$

Notice that full discrete scheme (32) does not require $P_h u(t_0) = u_h^0$. Below, we first present a lemma to derive stability analysis.

Lemma 3.5. *Let $\{v^j\}_{j=0}^m$ denote arbitrary series. Then for $m = 1, 2, \dots, n$, one has*

$$\begin{aligned} \mathcal{A}_h(v^m, \sum_{k=1}^m \bar{c}_{n,k} (v^k - v^{k-1})) &\geq \frac{1}{2} \sum_{k=1}^m \bar{c}_{n,k} (\mathcal{A}_h(v^k, v^k) - \mathcal{A}_h(v^{k-1}, v^{k-1})), \\ (v^m, \sum_{k=1}^m \bar{c}_{n,k} (v^k - v^{k-1})) &\geq \|v^m\| \sum_{k=1}^m \bar{c}_{n,k} (\|v^k\| - \|v^{k-1}\|), \end{aligned}$$

where $\mathcal{A}_h(\cdot, \cdot)$ is defined in Lemma 3.3, and $n = 1, 2, \dots, N$.

Proof. We temporarily let

$$H_m = \mathcal{A}_h(v^m, \sum_{k=1}^m \bar{c}_{n,k} (v^k - v^{k-1})) - \frac{1}{2} \sum_{k=1}^m \bar{c}_{n,k} (\mathcal{A}_h(v^k, v^k) - \mathcal{A}_h(v^{k-1}, v^{k-1})).$$

Then it just needs to show that $H_m \geq 0$. Since case $m = 1$ is clear, we discuss $m \geq 2$, namely,

$$\begin{aligned}
H_m &= \sum_{k=1}^m \bar{c}_{n,k} \mathcal{A}_h \left(v^k - v^{k-1}, \frac{1}{2} (v^k - v^{k-1}) + \sum_{s=k+1}^m (v^s - v^{s-1}) \right) \\
&= \frac{1}{2} \sum_{k=1}^m \bar{c}_{n,k} \mathcal{A}_h (v^k - v^{k-1}, v^k - v^{k-1}) + \sum_{k=1}^{m-1} \bar{c}_{n,k} \mathcal{A}_h \left(v^k - v^{k-1}, \sum_{s=k+1}^m (v^s - v^{s-1}) \right) \\
&= \frac{1}{2} \sum_{k=1}^m \bar{c}_{n,k} \mathcal{A}_h (v^k - v^{k-1}, v^k - v^{k-1}) + \sum_{s=1}^m \mathcal{A}_h \left(v^s - v^{s-1}, \sum_{k=1}^{s-1} \bar{c}_{n,k} (v^k - v^{k-1}) \right), \tag{34}
\end{aligned}$$

where the last equality used the following fact

$$\sum_{k=1}^{m-1} \mathcal{A}_h \left(z^k, \sum_{s=k+1}^m w^s \right) = \sum_{s=1}^m \mathcal{A}_h \left(w^s, \sum_{k=1}^{s-1} z^k \right).$$

Now we let $z^0 = 0$, and $z^k - z^{k-1} = (v^k - v^{k-1}) \bar{c}_{n,k}$ for $k = 1, 2, \dots, n$. From (34) we derive

$$\begin{aligned}
H_m &= \frac{1}{2} \sum_{k=1}^m \frac{1}{\bar{c}_{n,k}} \mathcal{A}_h (z^k - z^{k-1}, z^k - z^{k-1}) + \sum_{s=1}^m \frac{1}{\bar{c}_{n,s}} \mathcal{A}_h (z^s - z^{s-1}, z^{s-1}) \\
&= \frac{1}{2} \sum_{k=1}^{m-1} \left(\frac{1}{\bar{c}_{n,k}} - \frac{1}{\bar{c}_{n,k+1}} \right) \mathcal{A}_h (z^k, z^k) + \frac{1}{2} \frac{1}{\bar{c}_{n,m}} \mathcal{A}_h (z^m, z^m) \geq 0.
\end{aligned}$$

However, the second conclusion can be obtained by a direct expansion and the use of Cauchy-Schwarz inequality. Hence, we complete this proof of the lemma. \square

Theorem 3.1. Assume that $u_h^n \in V_h^d$ corresponds to the solution of full discrete scheme (32) using (33). Then we have

$$\|u_h^n\| \leq \frac{1}{\bar{c}_{n,n}} \left(\|f^n\| + \bar{c}_{n,1} \|u_h^0\| + \sum_{k=1}^{n-1} (\bar{c}_{n,k+1} - \bar{c}_{n,k}) \|u_h^k\| \right), \quad n = 1, 2, \dots, N,$$

where $1/\bar{c}_{n,n} = \tau_n$.

Proof. From (32), we take $v_h = u_h^n$ and invoke Lemma 3.5, then it follows that

$$\|u_h^n\| \sum_{k=1}^n \bar{c}_{n,k} (\|u_h^k\| - \|u_h^{k-1}\|) + \kappa_s \mathcal{A}_h (u_h^n, u_h^n) \leq (\bar{\partial}_t^\alpha u_h^n, u_h^n) + \kappa_s \mathcal{A}_h (u_h^n, u_h^n) = (f^n, u_h^n).$$

The uses of Cauchy-Schwarz inequality and positivity of $\mathcal{A}_h(\cdot, \cdot)$ give

$$\sum_{k=1}^n \bar{c}_{n,k} (\|u_h^k\| - \|u_h^{k-1}\|) \leq \|f^n\|, \quad n = 1, 2, \dots, N.$$

After a simple recombination of the above inequality yields the L^2 stability estimate. \square

Below is an L^2 stability with respect to a weighted sum. Then we define

$$\theta_{n,n} = 1, \quad \text{and} \quad \theta_{n,j} = \Gamma(2 - \alpha) \sum_{k=j}^{n-1} \Delta t_k^\alpha \theta_{k,j} (\bar{c}_{n,k+1} - \bar{c}_{n,k}), \quad j = 1, 2, \dots, n-1.$$

Theorem 3.2. Suppose that $u_h^n \in V_h^d$ denotes the solution of full discrete scheme (32). Then we have

$$\|u_h^n\| \leq \|u_h^0\| + \frac{1}{\bar{c}_{n,n}} \sum_{j=1}^n \theta_{n,j} \|f^j\|,$$

where $1/\bar{c}_{n,n} = \tau_n$, and $n = 1, 2, \dots, N$.

Proof. To complete this proof, we now apply mathematical induction on k , $k = 1, 2, \dots, n$. When $k = 1$ it is clear. Assume that conclusion holds for $k = 1, 2, \dots, n-1$. Then invoking Theorem 3.1, we shall obtain

$$\begin{aligned} \|u_h^n\| &\leq \frac{1}{\bar{c}_{n,n}} \left(\|f^n\| + \bar{c}_{n,1} \|u_h^0\| + \sum_{k=1}^{n-1} (\bar{c}_{n,k+1} - \bar{c}_{n,k}) \|u_h^k\| \right) \\ &\leq \frac{1}{\bar{c}_{n,n}} \left(\|f^n\| + \bar{c}_{n,n} \|u_h^0\| + \Gamma(2-\alpha) \sum_{j=1}^{n-1} \sum_{k=j}^{n-1} (\bar{c}_{n,k+1} - \bar{c}_{n,k}) \theta_{k,j} \Delta t_k^\alpha \|f^j\| \right) \\ &= \frac{1}{\bar{c}_{n,n}} \left(\|f^n\| + \bar{c}_{n,n} \|u_h^0\| + \sum_{j=1}^{n-1} \theta_{n,j} \|f^j\| \right), \end{aligned}$$

where the second line is obtained using equality

$$\sum_{k=1}^{n-1} w_{n,k} \sum_{j=1}^k z_{k,j} = \sum_{j=1}^{n-1} \sum_{k=j}^{n-1} w_{n,k} z_{k,j}.$$

Therefore, we get the desired result. \square

Theorem 3.2 shows that the stability bound shall not blow up as $\alpha \rightarrow 1^-$. To obtain the error estimate for full discrete scheme based on fast time-stepping scheme on graded mesh, we also need to provide an useful lemma. Though the definition of $\theta_{n,j}$ is different from direct L1 case in [50, Lemma 5.3, Corollary 5.4, Corollary 5.5], we can derive the following results.

Lemma 3.6. Assume $1 \leq \omega \leq 2(2-\alpha)/\alpha$, and let $n = 1, 2, \dots, N$. (a) Then for $\eta \in (0, 1)$, we can have

$$\Delta t_n^\alpha \sum_{j=1}^n j^{\omega(\eta-\alpha)} \theta_{n,j} \leq \frac{\Gamma(1-\alpha)}{\Gamma(2-\alpha)} \left(\frac{t_n}{T} \right)^\eta N^{\omega(\eta-\alpha)} T^\alpha.$$

(b) When taking $\eta = \alpha$ in (a), one has

$$\Delta t_n^\alpha \sum_{j=1}^n \theta_{n,j} \leq \frac{\Gamma(1-\alpha)}{\Gamma(2-\alpha)} t_n^\alpha.$$

(c) Denote $m^* = \{2-\alpha, \omega\alpha\}$, and choose $\eta = \delta + \alpha - \frac{m^*}{\omega}$ for $\delta \in (0, 1 - \frac{\alpha}{2})$. There holds

$$\Delta t_n^\alpha \sum_{j=1}^n j^{-m^*} \theta_{n,j} \leq \frac{\Gamma(1-\alpha)}{\Gamma(2-\alpha)} N^{\omega\delta} T^\alpha \left(\frac{t_n}{T} \right)^{\delta+\alpha-\frac{m^*}{\omega}} N^{-m^*}.$$

Proof. We now start to prove (a). Since $\bar{c}_{j,k} \geq \frac{t_j^{-\alpha}}{\Gamma(1-\alpha)}$ for $k = 1, 2, \dots, j$, we can derive

$$\bar{\partial}_t^\alpha t_j^\eta = \sum_{k=1}^j \bar{c}_{j,k} (t_k^\eta - t_{k-1}^\eta) = \eta \sum_{k=1}^j \bar{c}_{j,k} \int_{t_{k-1}}^{t_k} \zeta^{\eta-1} d\zeta \geq \frac{t_j^{\eta-\alpha}}{\Gamma(1-\alpha)}, \quad j = 1, 2, \dots, n.$$

Multiplying the above inequality by $\theta_{n,j}$, and summing from $j = 1$ to n yield

$$\begin{aligned} \frac{1}{\Gamma(1-\alpha)} \sum_{j=1}^n t_j^{\eta-\alpha} \theta_{n,j} &\leq \sum_{j=1}^n \theta_{n,j} \sum_{k=1}^j \bar{c}_{j,k} (t_k^\eta - t_{k-1}^\eta) = \sum_{k=1}^n (t_k^\eta - t_{k-1}^\eta) \sum_{j=k}^n \bar{c}_{j,k} \theta_{n,j} \\ &= \frac{1}{\Delta t_n^\alpha \Gamma(2-\alpha)} \sum_{k=1}^n (t_k^\eta - t_{k-1}^\eta) = \frac{t_n^\eta}{\Delta t_n^\alpha \Gamma(2-\alpha)}, \end{aligned} \quad (35)$$

where we used mathematical induction to prove

$$\frac{1}{\Delta t_n^\alpha \Gamma(2-\alpha)} = \sum_{j=k}^n \bar{c}_{j,k} \theta_{n,j}, \quad 1 \leq k \leq n.$$

Then we obtain (a) in terms of $t_j = \left(\frac{j}{N}\right)^\omega T$. The conclusion (b) is clear and the proof of (c) similarly follows from [50, Corollary 5.5]. \square

To explain why we consider graded time mesh and use the following time regularity assumption in the present temporal convergence analysis, a reason is illustrated in Appendix. Now, we shall give the following time regularity assumption.

Assumption 1. [50, 51] Let initial condition u_0 and right hand side function f in problem (1) satisfy appropriate conditions such that the solution u in (28) of (1) has

$$\|\partial_t^l u\|_q \leq C (1 + t^{\alpha-l}), \quad t > 0,$$

where C is a positive constant, $l = 0, 1, 2$, and q denotes non-negative integer number.

Analogous to [43, Lemma 2.6], using [51, Lemma 5.2], Assumption 1 and triangle inequality, we can bound

$$\|r^n\|_q \leq C \left(n^{-\min\{2-\alpha, \omega\alpha\}} + \epsilon \right), \quad n = 1, 2, \dots, N; \quad q = 0, 1, \quad (36)$$

where r^n denotes the truncation error of fast time-stepping L1 scheme in (24), ϵ is given in (22) to satisfy (21), and C is a positive constant.

We next extend the technique developed in [32] to time-space fractional diffusion problem with inhomogenous initial value and right hand side term. For simplicity, we temporarily denote $u_j(t) := (u(\cdot, t), \varphi_j)$, $f_j(t) := (f(\cdot, t), \varphi_j)$ and $u_{0j} := (u_0(\cdot), \varphi_j)$.

Theorem 3.3. Suppose that $\nu_0 = \sum_{j=1}^{\infty} |u_{0j}| (\lambda_j + \gamma)^{\frac{r+1}{2}+s} < \infty$ and $\nu_1 = \sup_{0 \leq t \leq T} \sum_{j=1}^{\infty} (\lambda_j + \gamma)^{\frac{r+1}{2}} |f_j(t)| < \infty$. If $u(t)$ in (28) is the solution of (1), then we have

$$|((-\Delta + \gamma \mathbb{I})^s u(t) - (-\Delta_h + \gamma \mathbb{I})^s P_h u(t), v_h)| \leq C (\nu_0 + \nu_1) h^{r+1} \|v_h\|, \quad \forall v_h \in V_h^d,$$

for $t > 0$, where C is a positive constant.

Proof. By Lemma 3.1 and Lemma 3.2, we have

$$\begin{aligned} |u_j(t)| &= \left| u_{0j} E_{\alpha,1}(-\kappa_s (\lambda_j + \gamma)^s t^\alpha) + \int_0^t (t-\tau)^{\alpha-1} E_{\alpha,\alpha}(-\kappa_s (\lambda_j + \gamma)^s (t-\tau)^\alpha) f_j(\tau) d\tau \right| \\ &\leq |u_{0j}| \frac{C_1}{1 + \kappa_s (\lambda_j + \gamma)^s t^\alpha} + \sup_{0 \leq \tau \leq T} |f_j(\tau)| \left| \int_0^t (t-\tau)^{\alpha-1} E_{\alpha,\alpha}(-\kappa_s (\lambda_j + \gamma)^s (t-\tau)^\alpha) d\tau \right| \\ &\leq C_1 |u_{0j}| + \frac{C_2}{(\lambda_j + \gamma)^s} \sup_{0 \leq \tau \leq T} |f_j(\tau)|, \quad \forall t > 0. \end{aligned} \quad (37)$$

In addition, the H^{r+1} -norm of φ_j satisfies the following growth condition:

$$\|\varphi_j\|_{r+1} \leq C \lambda_j^{\frac{r+1}{2}} \leq C (\lambda_j + \gamma)^{\frac{r+1}{2}}, \quad \forall j \in \mathbb{N}^+. \quad (38)$$

Hence, using (37), (38) and Lemma 3.3, we can derive the estimate

$$\begin{aligned} |(((-\Delta + \gamma \mathbb{I})^s - (-\Delta_h + \gamma \mathbb{I})^s P_h) u(t), v_h)| &\leq \sum_{j=1}^{\infty} |(u_j(t) ((-\Delta + \gamma \mathbb{I})^s - (-\Delta_h + \gamma \mathbb{I})^s P_h) \varphi_j, v_h)| \\ &\leq Ch^{r+1} \|v_h\| \sum_{j=1}^{\infty} \|\varphi_j\|_k |u_j(t)| (\lambda_j + \gamma)^s \leq Ch^{r+1} \|v_h\| \sum_{j=1}^{\infty} |u_j(t)| (\lambda_j + \gamma)^{\frac{r+1}{2} + s} \\ &\leq Ch^{r+1} \|v_h\| (\nu_0 + \nu_1), \quad \forall v_h \in V_h^d. \end{aligned}$$

This completes the proof. \square

Theorem 3.4. *Let $u(t)$ be the solution of (1) satisfying regularity in Assumption 1, graded mesh factor $\omega \leq 2(2 - \alpha)/\alpha$, and $u(t_n) \in H^{r+1}(\Omega)$ for $n = 0, 1, \dots, N$. Under the assumptions of Theorem 3.3 and Lemma 3.6, the full discrete scheme (32) has the following error estimate*

$$\max_{1 \leq n \leq N} \|u(t_n) - u_h^n\| \leq C \left(N^{-\{2-\alpha, \omega\alpha\}} + h^{r+1} + \|u(t_0) - u_h^0\| + \epsilon \right),$$

where C corresponds to a positive constant, and ϵ is given in (22) to satisfy (21) and it is small sufficiently enough to be ignored.

Proof. We first derive semi-discrete scheme for simplicity of analysis. Find $u(t_n) \in \dot{H}^{2s}(\Omega)$ such that

$$(\partial_t^\alpha u(t_n), v_h) + \kappa_s ((-\Delta + \gamma \mathbb{I})^s u(t_n), v_h) = (f^n, v_h), \quad \forall v_h \in V_h^d, \quad (39)$$

where $f^n = f(\cdot, t_n)$. According to (39), we immediately have

$$\begin{aligned} (\bar{\partial}_t^\alpha P_h u(t_n), v_h) + \kappa_s ((-\Delta_h + \gamma \mathbb{I})^s P_h u(t_n), v_h) \\ = ((\bar{\partial}_t^\alpha - \partial_t^\alpha) u(t_n), v_h) + (f^n, v_h) + (\bar{\partial}_t^\alpha (P_h - \mathbb{I}) u(t_n), v_h) \\ + \kappa_s (((-\Delta_h + \gamma \mathbb{I})^s P_h - (-\Delta + \gamma \mathbb{I})^s) u(t_n), v_h), \quad \forall v_h \in V_h^d. \end{aligned} \quad (40)$$

Combining (33), (30) and Assumption 1 with $q = r + 1$ and $l = 1$ easily gives

$$\begin{aligned} \|\bar{\partial}_t^\alpha (P_h - \mathbb{I}) u(t_n)\| &\leq Ch^{r+1} \sum_{k=1}^n \bar{c}_{n,k} \int_{t_{k-1}}^{t_k} \|u_\tau\|_{r+1} d\tau \leq Ch^{r+1} \sum_{k=1}^n \bar{c}_{n,k} \int_{t_{k-1}}^{t_k} \tau^{\alpha-1} d\tau, \\ &\leq Ch^{r+1} \bar{c}_{n,n} \int_0^{t_n} \tau^{\alpha-1} d\tau = Ch^{r+1}. \end{aligned} \quad (41)$$

Now, denoting $\rho^n = P_h u(t_n) - u_h^n$, and subtracting (32) from (40), we have

$$\begin{aligned} (\bar{\partial}_t^\alpha \rho^n, v_h) + \kappa_s ((-\Delta_h + \gamma \mathbb{I})^s \rho^n, v_h) &= ((\bar{\partial}_t^\alpha - \partial_t^\alpha) u(t_n), v_h) + (\bar{\partial}_t^\alpha (P_h - \mathbb{I}) u(t_n), v_h) \\ &\quad + \kappa_s (((-\Delta_h + \gamma \mathbb{I})^s P_h - (-\Delta + \gamma \mathbb{I})^s) u(t_n), v_h), \quad \forall v_h \in V_h^d. \end{aligned} \quad (42)$$

However, due to the use of Theorem 3.3, we can not directly invoke stability estimate established in Theorem 3.2 to bound ρ^n . Hence, we have to return back to the proof of Theorem 3.1 by considering (42).

Similar to Theorem 3.1, taking $v_h = \rho^n$ in (42) and invoking Theorem 3.3, we have

$$\begin{aligned} \|\rho^n\| \sum_{k=1}^n \bar{c}_{n,k} (\|\rho^k\| - \|\rho^{k-1}\|) &\leq \|(\bar{\partial}_t^\alpha - \partial_t^\alpha) u(t_n)\| \|\rho^n\| + \|\bar{\partial}_t^\alpha (P_h - \mathbb{I}) u(t_n)\| \|\rho^n\| \\ &\quad + C\kappa_s (\nu_0 + \nu_1) h^{r+1} \|\rho^n\| =: \|z^n\| \|\rho^n\|, \end{aligned} \quad (43)$$

where C , ν_0 and ν_1 are three constants given by Theorem 3.3. Hence, eliminating $\|\rho^n\|$ in (43) yields

$$\|\rho^n\| \leq \frac{1}{\bar{c}_{n,n}} \left(\|z^n\| + \bar{c}_{n,1} \|\rho^0\| + \sum_{k=1}^{n-1} (\bar{c}_{n,k+1} - \bar{c}_{n,k}) \|\rho^k\| \right), \quad n = 1, 2, \dots, N.$$

A same technique in Theorem 3.2 derives

$$\|\rho^n\| \leq \|\rho^0\| + \Delta t_n^\alpha \Gamma(2 - \alpha) \sum_{j=1}^n \theta_{n,j} \|z^j\|, \quad n = 1, 2, \dots, N. \quad (44)$$

Next, we are ready to bound $\|\rho^n\|$. Substituting $\|z^j\|$ in (43) into (44) leads to

$$\begin{aligned} \|\rho^n\| &\leq \|\rho^0\| + \frac{1}{\bar{c}_{n,n}} \sum_{j=1}^n \theta_{n,j} \|(\bar{\partial}_t^\alpha - \partial_t^\alpha) u(t_j)\| + \frac{1}{\bar{c}_{n,n}} \sum_{j=1}^n \theta_{n,j} \|\bar{\partial}_t^\alpha (P_h - \mathbb{I}) u(t_j)\| \\ &\quad + C\kappa_s (\nu_0 + \nu_1) h^{r+1} \frac{1}{\bar{c}_{n,n}} \sum_{j=1}^n \theta_{n,j} \\ &\leq \|\rho^0\| + C \Delta t_n^\alpha \sum_{j=1}^n \theta_{n,j} j^{-\{2-\alpha, \omega\alpha\}} + C (h^{r+1} + \epsilon) \Delta t_n^\alpha \sum_{j=1}^n \theta_{n,j} \\ &\leq \|\rho^0\| + C \left(N^{-\{2-\alpha, \omega\alpha\}} + h^{r+1} + \epsilon \right), \quad n = 1, 2, \dots, N, \end{aligned} \quad (45)$$

where we also used (36), (41) and Lemma 3.6. By triangle inequality we will also obtain

$$\|\rho^0\| \leq \|P_h u(t_0) - u(t_0)\| + \|u(t_0) - u_h^0\| \leq Ch^{r+1} \|u(t_0)\|_{r+1} + \|u(t_0) - u_h^0\|. \quad (46)$$

Hence, combining (30), (45) and (46), and using

$$\max_{1 \leq n \leq N} \|u(t_n) - u_h^n\| \leq \max_{1 \leq n \leq N} \|u(t_n) - P_h u(t_n)\| + \max_{1 \leq n \leq N} \|\rho^n\|,$$

we immediately prove the desired result. \square

From Theorem 3.4, we can notice that the choice of $\omega = (2 - \alpha)/\alpha$ shall yield an optimal temporal convergence $\mathcal{O}(N^{-(2-\alpha)})$, but the error bound is α -nonrobust as $\alpha \rightarrow 1^-$ due to the use of Lemma 3.6. For the convergence analysis of full discrete scheme (26) employing fourth-order CDM, a similar discussion can be seen in [29]. Next, we shall provide some numerical examples to illustrate our theoretical achievements.

4. Numerical experiments

In this section, several numerical examples are delivered to test the performance of the present fast algorithm for fractional diffusion equations with spectral fractional Laplacian. Also, all numerical simulations are conducted using Python 3.7 on the personal computer.

Table 1: The L^2 error and the corresponding convergence rate of Example 1 in linear FEM.

(s, γ)	\mathcal{M}	8	16	32	64	128	256
(0.4, 0)	$\ e_h\ _2$	1.746E-02	3.908E-03	9.507E-04	2.361E-04	5.892E-05	1.472E-05
	r_2		2.160	2.039	2.010	2.002	2.001
(1.2, 0)	$\ e_h\ _2$	3.218E-04	7.312E-05	1.786E-05	4.438E-06	1.108E-06	2.769E-07
	r_2		2.138	2.034	2.008	2.002	2.001
(0.8, 1)	$\ e_h\ _2$	2.365E-03	5.332E-04	1.300E-04	3.229E-05	8.059E-06	2.014E-06
	r_2		2.149	2.037	2.009	2.002	2.001
(1.6, 1)	$\ e_h\ _2$	4.282E-05	9.802E-06	2.398E-06	5.962E-07	1.489E-07	3.720E-08
	r_2		2.127	2.031	2.008	2.002	2.001
(1.0, 2)	$\ e_h\ _2$	8.639E-04	1.955E-04	4.770E-05	1.185E-05	2.959E-06	7.394E-07
	r_2		2.144	2.035	2.009	2.002	2.001
(2.0, 2)	$\ e_h\ _2$	5.628E-06	1.297E-06	3.179E-07	7.909E-08	1.975E-08	4.936E-09
	r_2		2.117	2.029	2.007	2.002	2.001

Table 2: L^2 errors and the corresponding convergence rates of Example 1 in fourth-order CDM.

(s, γ)	\mathcal{M}	8	16	32	64	128	256
(0.3, 0)	$\ e_h\ _2$	4.113E-05	2.525E-06	1.571E-07	9.806E-09	6.127E-10	3.829E-11
	r_2		4.026	4.007	4.002	4.000	4.000
(1.3, 0)	$\ e_h\ _2$	1.506E-06	9.238E-08	5.747E-09	3.588E-10	2.242E-11	1.401E-12
	r_2		4.027	4.007	4.002	4.000	4.000
(0.5, 1)	$\ e_h\ _2$	2.606E-05	1.599E-06	9.949E-08	6.211E-09	3.881E-10	2.425E-11
	r_2		4.026	4.007	4.002	4.000	4.000
(1.5, 1)	$\ e_h\ _2$	6.550E-07	4.017E-08	2.499E-09	1.560E-10	9.748E-12	6.092E-13
	r_2		4.027	4.007	4.002	4.000	4.000
(0.7, 2)	$\ e_h\ _2$	1.382E-05	8.481E-07	5.276E-08	3.294E-09	2.058E-10	1.286E-11
	r_2		4.026	4.007	4.002	4.000	4.000
(1.7, 2)	$\ e_h\ _2$	2.789E-07	1.710E-08	1.064E-09	6.642E-11	4.150E-12	2.594E-13
	r_2		4.028	4.007	4.001	4.000	4.000

4.1. Accuracy test

To check the accuracy and efficiency of the present algorithm, we first study the high dimensional fractional Poisson problem (4). Unless otherwise specified, $\Omega = (0, 1)^d$, $\mathcal{M} = N_1 = \dots = N_d$, $h = \mathcal{M}^{-1}$ and $\mathbf{x} = (x_1, x_2, \dots, x_d)$ are given throughout numerical section.

From the definition of $(-\Delta + \gamma \mathbb{I})^s$, it will be convenient to construct the exact solution by replacing j with (i_1, i_2, \dots, i_d) in (3). Hence the exact solution of (4) can be easily expressed as

$$u(\mathbf{x}) = \sum_{i_1, i_2, \dots, i_d=1}^{\infty} (\lambda_{i_1, i_2, \dots, i_d} + \gamma)^{-s} \widehat{f}_{i_1, i_2, \dots, i_d} \varphi_{i_1, i_2, \dots, i_d}(\mathbf{x}), \quad \forall \mathbf{x} \in \bar{\Omega}, \quad (47)$$

where the coefficients

$$\widehat{f}_{i_1, i_2, \dots, i_d} = \int_{\Omega} f(\mathbf{x}) \varphi_{i_1, i_2, \dots, i_d}(\mathbf{x}) d\mathbf{x}, \quad i_1, i_2, \dots, i_d \in \mathbb{N}^+.$$

Besides, we choose the eigenpairs of Laplacian operator $(-\Delta)$ as follows:

$$\lambda_{i_1, i_2, \dots, i_d} = \pi^2 \sum_{k=1}^d i_k^2, \quad \text{and} \quad \varphi_{i_1, i_2, \dots, i_d}(\mathbf{x}) = 2 \prod_{k=1}^d \sin(i_k \pi x_k), \quad i_1, i_2, \dots, i_d \in \mathbb{N}^+.$$

From (47), the exact solution $u(\mathbf{x})$ can be constructed by taking appropriate $f(\mathbf{x})$.

Example 1. (Smooth solution) Taking $f(\mathbf{x}) = \prod_{k=1}^d \sin(n\pi x_k)$ in equation (4) leads to

$$\hat{f}_{i_1, i_2, \dots, i_d} = \frac{1}{2} \prod_{k=1}^d \left(\frac{\sin(n\pi - i_k\pi)}{n\pi - i_k\pi} - \frac{\sin(n\pi + i_k\pi)}{n\pi + i_k\pi} \right), \quad n \in \mathbb{N}^+.$$

It can be found that $\hat{f}_{i_1, i_2, \dots, i_d}$ is $\frac{1}{2}$ in the sense of limitation if $i_1 = i_2 = \dots = i_d = n$; otherwise, it will vanish. Hence we have from (47) that

$$u(\mathbf{x}) = \frac{1}{(dn^2\pi^2 + \gamma)^s} \prod_{k=1}^d \sin(n\pi x_k), \quad n \in \mathbb{N}^+.$$

In Example 1, we take $n = 2$ and $d = 3$. The error is measured by $\|e_h\|_2 = \|u - u_h\|$ in L^2 -norm, and the convergence rate is computed by $r_2 = \log_2 \left(\frac{\|e_h\|_2}{\|e_{h/2}\|_2} \right)$. Hence the expected accuracy is second order in linear FEM, and the expected accuracy is fourth order in CDM. The results are shown in Tables 1 and 2.

Example 2. (Singular solution) Let $f(\mathbf{x}) = 1$, $\gamma = 1$ and $d = 2$ in (4).

Table 3: L^2 errors and the convergence rates of Example 2 in FEM and CDM.

s	\mathcal{M}	FEM	r_2	CDM	r_2	s	\mathcal{M}	FEM	r_2	CDM	r_2
0.5	64	3.996E-04		3.039E-04		0.9	64	1.984E-05		4.232E-05	
	128	1.377E-04	1.537	1.089E-04	1.480		128	4.935E-06	2.008	1.098E-05	1.946
	256	4.798E-05	1.521	3.879E-05	1.490		256	1.231E-06	2.003	2.810E-06	1.966
	512	1.682E-05	1.512	1.376E-05	1.495		512	3.075E-07	2.001	7.131E-07	1.979
	1024	5.920E-06	1.507	4.873E-06	1.498		1024	7.684E-08	2.001	1.800E-07	1.986
	2048	2.088E-06	1.504	1.725E-06	1.499		2048	1.921E-08	2.000	4.528E-08	1.991
1.3	64	3.649E-06		1.007E-05		1.7	64	5.738E-07		2.860E-06	
	128	9.124E-07	2.000	2.524E-06	1.997		128	1.436E-07	1.999	7.155E-07	1.995
	256	2.281E-07	2.000	6.313E-07	1.999		256	3.590E-08	2.000	1.789E-07	2.000
	512	5.702E-08	2.000	1.579E-07	2.000		512	8.976E-09	2.000	4.473E-08	2.000
	1024	1.425E-08	2.000	3.947E-08	2.000		1024	2.244E-09	2.000	1.118E-08	2.000
	2048	3.563E-09	2.000	9.867E-09	2.000		2048	5.610E-10	2.000	2.796E-09	2.000

In Example 2, the L^2 error can be measured by $\|e_h\|_2 = \|u_h - u_{h/2}\|$, the convergence rate is given by $r_2 = \log_2 \left(\frac{\|e_h\|_2}{\|e_{h/2}\|_2} \right)$, and the expected accuracy is $\mathcal{O}(h^{2s+\frac{1}{2}})$ and $\mathcal{O}(h^2)$ for $s < 0.75$ and $s \geq 0.75$, respectively. The numerical results are presented in Table 3, and the numerical accuracy is consistent with [30]. It is noteworthy that the error is measured in L^2 -norm, however, the numerical accuracy will be $\mathcal{O}(h^{2s})$ for $s \in (0, 1)$ if using L^∞ -norm to measure the error.

4.2. Time-dependent problems

In this subsection, we shall apply the present double fast algorithm to time-space fractional diffusion problems. To this end, we also take $Q = 128$ and $\epsilon = 10^{-16}$ in (20).

Example 3. Let g be time-dependent smooth function, and assume that the exact solution of (1)

$$u(\mathbf{x}, t) = \frac{g(t)}{(dn^2\pi^2 + \gamma)^s} \prod_{k=1}^d \sin(n\pi x_k), \quad n \in \mathbb{N}^+,$$

is chosen so that

$$f(\mathbf{x}, t) = \left(\frac{\partial_t^\alpha g(t)}{(dn^2\pi^2 + \gamma)^s} + \kappa_s g(t) \right) \prod_{k=1}^d \sin(n\pi x_k), \quad n \in \mathbb{N}^+.$$

In Example 3, we first take $d = 2$, $\gamma = 1$, $n = 1$, $\omega = 1$ and $\kappa_s = 0.1$. In addition, the L^∞ error is computed at $t_N = T$ and the spatial numerical method uses CDM. Then the spatial numerical results are presented in Table 4 with $g(t) = t$, $N = 5000$ is fixed, and the expected accuracy is $\mathcal{O}(h^4)$ in space. The temporal numerical results are shown in Table 5 with $g(t) = t^{1.5}$ and $\mathcal{M} = 500$, and the expected accuracy is $\mathcal{O}(\Delta t^{2-\alpha})$ in time.

Table 4: Spatial numerical errors and the convergence rates of Example 3 in L^∞ -norm.

(s, α)	\mathcal{M}	5	10	20	40	80
(1.0, 0.8)	$\ e_h\ _\infty$	1.650E-05	1.127E-06	7.021E-08	4.385E-09	2.740E-10
	r_∞		3.872	4.004	4.001	4.000
(0.8, 0.8)	$\ e_h\ _\infty$	1.747E-05	1.193E-06	7.437E-08	4.645E-09	2.902E-10
	r_∞		3.872	4.004	4.001	4.000
(0.8, 0.6)	$\ e_h\ _\infty$	1.861E-05	1.271E-06	7.920E-08	4.947E-09	3.090E-10
	r_∞		3.872	4.004	4.001	4.001
(0.6, 0.6)	$\ e_h\ _\infty$	1.730E-05	1.182E-06	7.363E-08	4.598E-09	2.872E-10
	r_∞		3.872	4.004	4.001	4.001
(0.6, 0.4)	$\ e_h\ _\infty$	1.869E-05	1.277E-06	7.955E-08	4.966E-09	3.087E-10
	r_∞		3.872	4.004	4.002	4.008
(0.4, 0.4)	$\ e_h\ _\infty$	1.459E-05	9.969E-07	6.212E-08	3.876E-09	2.386E-10
	r_∞		3.872	4.004	4.002	4.022

Table 5: Temporal numerical errors and the convergence rates of Example 3 in L^∞ -norm.

(s, α)	N	20	40	80	160	320
(1.0, 0.8)	$\ e_h\ _\infty$	1.963E-04	8.601E-05	3.761E-05	1.643E-05	7.168E-06
	r_∞		1.190	1.193	1.195	1.197
(0.8, 0.8)	$\ e_h\ _\infty$	5.746E-04	2.540E-04	1.117E-04	4.894E-05	2.140E-05
	r_∞		1.178	1.186	1.190	1.193
(0.8, 0.6)	$\ e_h\ _\infty$	2.013E-04	7.723E-05	2.951E-05	1.125E-05	4.280E-06
	r_∞		1.382	1.388	1.392	1.394
(0.6, 0.6)	$\ e_h\ _\infty$	5.165E-04	1.993E-04	7.643E-05	2.920E-05	1.113E-05
	r_∞		1.374	1.383	1.388	1.392
(0.6, 0.4)	$\ e_h\ _\infty$	1.653E-04	5.583E-05	1.874E-05	6.258E-06	2.084E-06
	r_∞		1.566	1.575	1.582	1.586
(0.4, 0.4)	$\ e_h\ _\infty$	3.802E-04	1.288E-04	4.333E-05	1.450E-05	4.833E-06
	r_∞		1.561	1.572	1.579	1.585

To illustrate the efficiency of the present double fast algorithm for solving time-space fractional diffusion problem in Example 3, we also provide a comparison of CPU time between fast L1 (fL1) scheme and direct L1 scheme. Here, the fast linear FEM (fFEM) and fast fourth-order CDM (fCDM) using discrete sine transform are carried out in space, respectively, $s = \alpha = 0.4$ is fixed and $g(t) = t^{1.5}$ is chosen.

From Table 6, we observed that the numerical accuracy of both L1 scheme and fL1 scheme are almost the same. For scheme using FEM, the error order exhibits $\mathcal{O}(h^2 + N^{-1})$, which is due to the fact that the

Table 6: A comparison of CPU time (seconds) between direct L1 and fast L1 for Example 3 with $\mathcal{M} \approx \sqrt{N}$.

Scheme	N	1000	2000	4000	8000	16000
fFEM-L1	$\ e_h\ _\infty$	1.841156E-05	9.292752E-06	4.570950E-06	2.305831E-06	1.155627E-06
	cpu (s)	2.286	10.47	60.76	422.4	2801
fFEM-FL1	$\ e_h\ _\infty$	1.841157E-05	9.292755E-06	4.570953E-06	2.305844E-06	1.155638E-06
	cpu (s)	1.168	5.473	22.84	116.2	394.9
fCDM-L1	$\ e_h\ _\infty$	7.974488E-07	2.641280E-07	8.715063E-08	2.878578E-08	9.505049E-09
	cpu (s)	2.322	10.64	60.13	393.7	2660
fCDM-FL1	$\ e_h\ _\infty$	7.974468E-07	2.641250E-07	8.714802E-08	2.877249E-08	9.493764E-09
	cpu (s)	1.182	5.357	21.58	112.0	449.9

Table 7: Optimal temporal numerical errors defined in Theorem 3.4 and the convergence orders of Example 3.

(α, ω)	N	20	40	80	160	320
(0.9, 1.222)	Error	8.574E-04	4.502E-04	2.3250E-04	1.185E-04	5.972E-05
	Order		0.9292	0.9533	0.9726	0.9884
(0.8, 1.500)	Error	1.074E-03	5.156E-04	2.427E-04	1.126E-04	5.161E-05
	Order		1.059	1.087	1.108	1.125
(0.7, 1.857)	Error	1.025E-03	4.506E-04	1.940E-04	8.223E-05	3.447E-05
	Order		1.186	1.216	1.238	1.254
(0.6, 2.333)	Error	8.860E-04	3.583E-04	1.419E-04	5.539E-05	2.142E-05
	Order		1.306	1.336	1.357	1.371
(0.5, 3.000)	Error	7.325E-04	2.743E-04	1.007E-04	3.655E-05	1.316E-05
	Order		1.417	1.445	1.463	1.473
(0.4, 4.000)	Error	5.932E-04	2.077E-04	7.158E-05	2.445E-05	8.302E-06
	Order		1.514	1.537	1.550	1.558

theoretical accuracy $\mathcal{O}(h^2 + N^{-1.6})$ and $h = N^{-0.5}$ lead to that the spatial convergence quickly reaches optimal order but the order is merely 1 in time. While for scheme employing CDM, the error order enjoys $\mathcal{O}(h^{3.2} + N^{-1.6})$. This is because the temporal convergence achieves optimal order $2 - \alpha$ early so that the order is not better than $4 - 2\alpha$ in space. For computational speed, the schemes using FL1 are significantly faster. These results demonstrate that the present double fast algorithm really can reduce the CPU time and save the memory.

Table 7 presents a set of temporal numerical results which are mainly to illustrate the Theorem 3.4. The choices of all parameters are same as Table 6. However, we shall consider a weak smooth time-dependent function $g(t) = t^\alpha$ in Example 3 satisfying time regularity Assumption 1 and also fix $\mathcal{M} = 100$ to obtain the desired convergence orders. It can be noted that the choice of graded temporal mesh factor $\omega = (2 - \alpha)/\alpha$ brought an optimal $\mathcal{O}(N^{-(2-\alpha)})$ convergence in time direction. Hence, these results are consistent with our theoretical analysis.

Example 4. In the example, we study the coarsening dynamics of the following time-space fractional phase-field problem

$$\begin{cases} \partial_t^\alpha u(\mathbf{x}, t) = -(-\Delta)^\beta (\varepsilon^{2s}(-\Delta + \gamma \mathbb{I})^s u(\mathbf{x}, t) + F(u)), & \mathbf{x} \in \Omega, t > 0, \\ u(\mathbf{x}, t) = g(\mathbf{x}, t), & \mathbf{x} \in \partial\Omega, t \geq 0, \\ u(\mathbf{x}, 0) = u_0(\mathbf{x}), & \mathbf{x} \in \Omega, \end{cases}$$

where u is the scaled concentration subject to the given initial value u_0 and boundary data g , the nonlinear term $F(u) = u^3 - u$, $0 < \alpha, s, \beta < 1$, $\gamma \geq 0$ and $\varepsilon > 0$ is an interfacial parameter describing the thickness of the phase boundary.

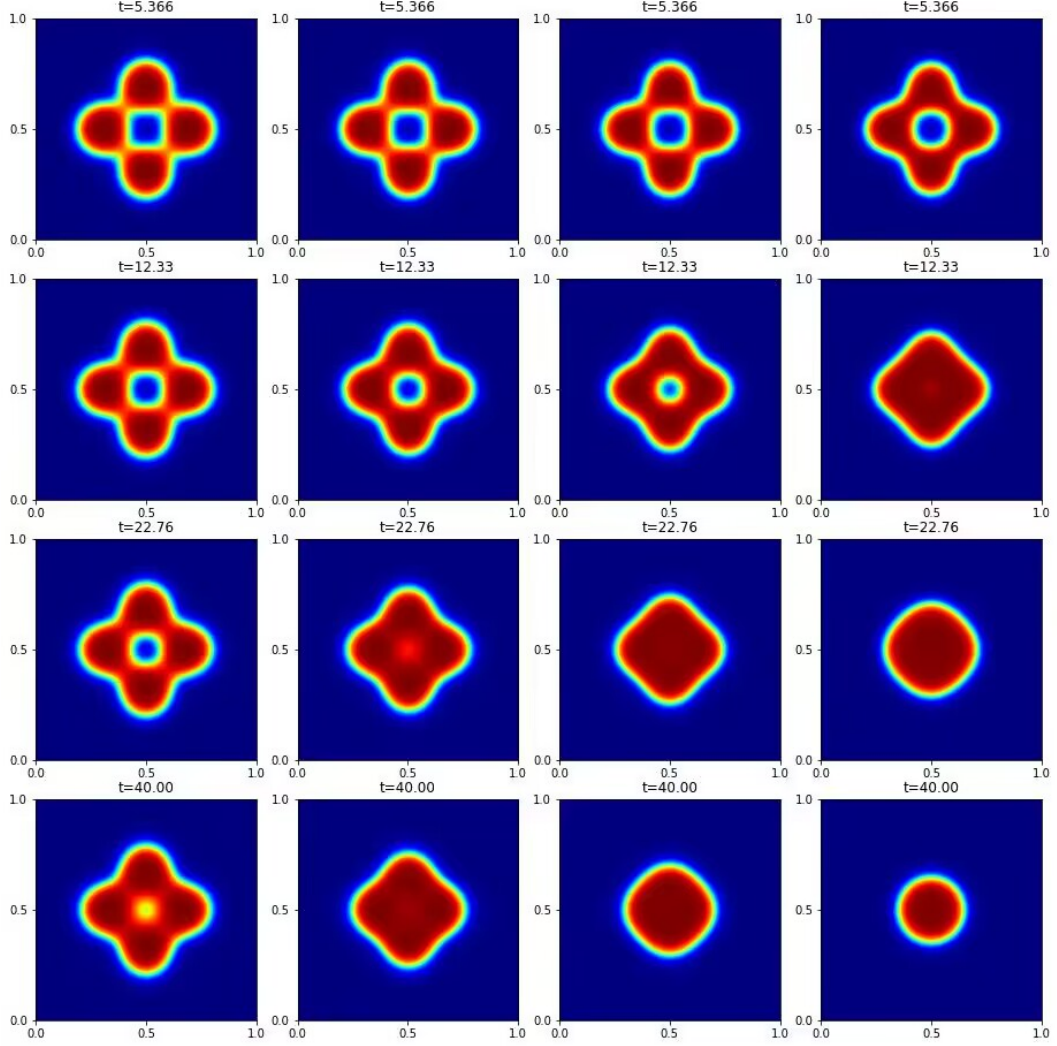


Figure 1: Process of the evolution of time-space fractional Allen-Cahn equation with the kissing bubbles: $\alpha = 0.4, 0.6, 0.8, 1$ from left to right, respectively.

In Example 4, fast time-stepping L1 method is used, and linear FEM for spatial discretization is performed.

We first consider $\beta = 0$, $\gamma = 1$, $\varepsilon = 0.02$ and $g(\mathbf{x}, t) = -1$ so that the Example 4 collapses to time-space fractional Allen-Cahn equation. Then we choose the initial value

$$u_0(\mathbf{x}) = -\prod_{i=1}^4 \tanh\left(\frac{|\mathbf{x} - \mathbf{x}_i|^2 - 0.015}{0.5\varepsilon}\right), \quad \mathbf{x} \in \Omega,$$

where $(x_1, y_1) = (0.7, 0.5)$, $(x_2, y_2) = (0.3, 0.5)$, $(x_3, y_3) = (0.5, 0.7)$ and $(x_4, y_4) = (0.5, 0.3)$. In addition, take $u = \bar{u} - 1$ such that the inhomogeneous Dirichlet boundary condition turns a homogeneous case.

In the numerical test, to investigate the process of the evolution of four kissing bubbles for $\alpha = 1, 0.8, 0.6, 0.4$ at different time level, we fix $s = 0.8$, $h = 2^{-10}$, $T = 40$, $N = 1600$ and $\omega = 1.2$. From Figure 1, we observed that four bubbles will shrink and turn into a single bubble with different rate of change, however, the process of the evolution of the bubble is slower for smaller α .

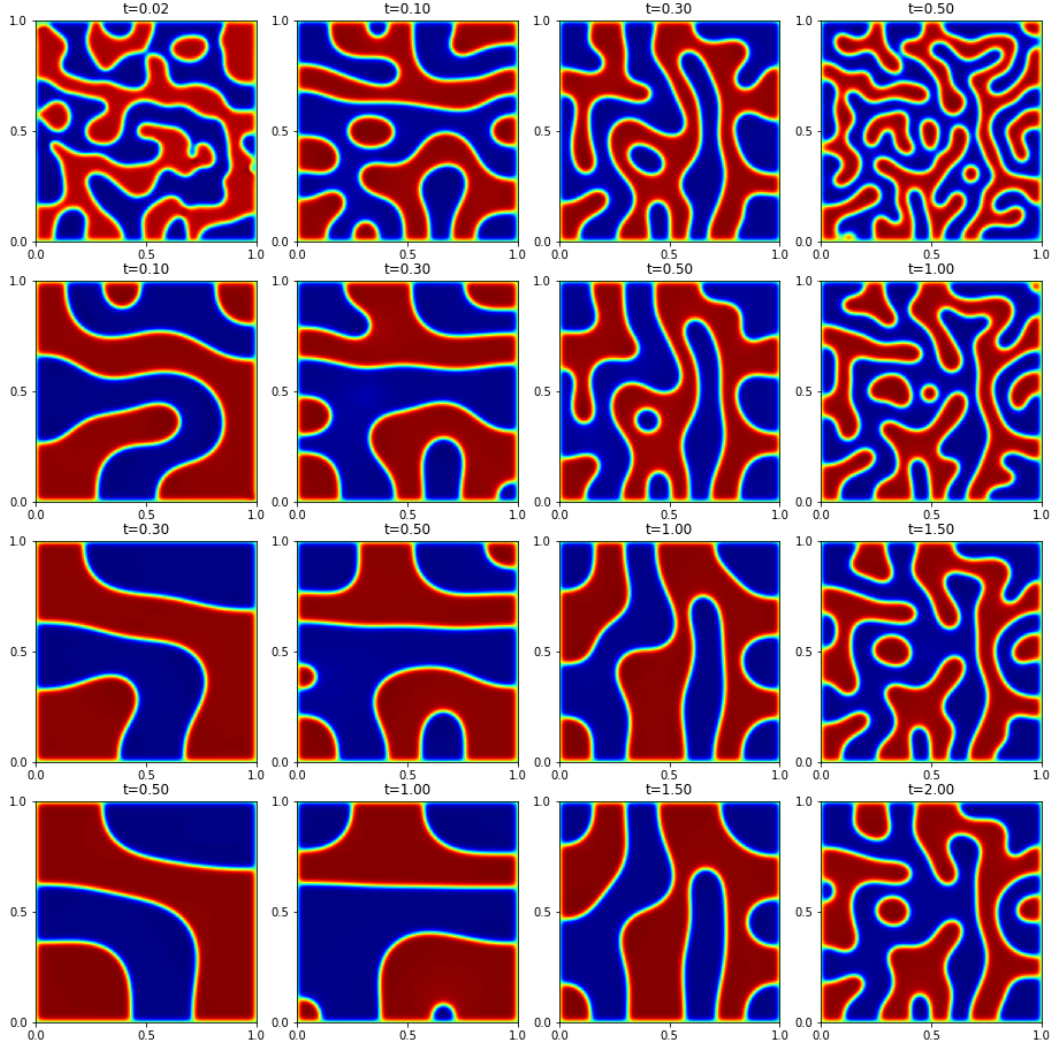


Figure 2: Snapshots of the numerical solutions of time-space fractional Cahn-Hilliard equation with $\beta = 1.0, 0.8, 0.6, 0.4$ from left to right, respectively.

Next, we study the time-space fractional Cahn-Hilliard equation in Example 4 with $s = 1$. Here, we choose initial value as a random perturbation uniformly distributed in $[-0.05, 0.05]^2$, and take $g(\mathbf{x}, t) = 0$, $\varepsilon = 0.01$, $\omega = 1$, $\alpha = 0.8$, $\Delta t = 0.001$ and $h = 2^{-9}$.

We consider different β to study the effect on coarsening behavior of the time-space fractional Cahn-Hilliard equation. Figure 2 shows the snapshots of the numerical solutions at different time for $\beta = 1.0, 0.8, 0.6$ and 0.4 from first column to last one, respectively, and the present numerical simulations use the same initial data. We found that the change of the states of solutions is significant, and the solutions would converge to different steady states for different values of β .

From Figures 1 and 2, we observed that the proposed double fast algorithm can efficiently simulate the time-space fractional phase-field models. Some similar simulations can be seen in [52].

5. Conclusion

In this paper, we proposed both commendably concise and implementation-friendly double fast algorithm for solving time-space fractional diffusion problems. We first employed linear finite element or fourth-order compact difference method combining with matrix transfer technique to approximate spectral fractional Laplacian, and then derived semi-discrete scheme of time-space fractional diffusion equation. In addition, a full discrete scheme using fast time-stepping L1 method on graded time mesh was provided, and then its α -robust stability and convergence analyses were discussed. Numerical simulations showed that the present algorithm really could reduce computation cost and memory requirement. For instance, $\mathcal{M} = 256$ and $\mathcal{M} = 1024$ were taken in Examples 1 and 4, the scales of algebraic matrix were over 16 million and one million, respectively. It is not realistic to obtain these results when using direct numerical methods.

Our spatial algorithm is based on specific Cartesian meshes, and thus may not be directly extended to more complex regions. The design on the corresponding fast algorithms remains open and certainly should be a subject of future research. In the end, since the use of Lemma 3.6, the error bound of Theorem 3.4 exhibits an α -nonrobust behavior, namely, the bound will blow up as $\alpha \rightarrow 1^-$.

Acknowledgments

The authors are very thankful to the editors and reviewers for carefully reading the paper, their suggestions and comments have improved the quality of the paper.

Data availability

Data will be made available on request.

Declarations

The authors declare that there is no conflict of interest.

Appendix

Here, we introduce a linear interpolation function of the solution $u(\zeta)$:

$$L_k(\zeta) = \frac{t_k - \zeta}{\Delta t} u(t_{k-1}) + \frac{\zeta - t_{k-1}}{\Delta t} u(t_k), \quad \zeta \in (t_{k-1}, t_k), \quad k = 1, 2, \dots, N,$$

where $\Delta t = t_k - t_{k-1}$. Define a second order difference quotient of $u(t)$ at t_{k-1} , t_k and ζ :

$$u[t_{k-1}, t_k, \zeta] = \frac{u[t_k, \zeta] - u[t_{k-1}, t_k]}{\zeta - t_{k-1}}, \quad \text{and} \quad u[t_i, t_j] = \frac{u(t_j) - u(t_i)}{t_j - t_i}.$$

According to Newton interpolation, we have

$$u(\zeta) = L_k(\zeta) + R_k(\zeta), \quad R_k(\zeta) = (\zeta - t_{k-1})(\zeta - t_k)u[t_{k-1}, t_k, \zeta], \quad \zeta \in (t_{k-1}, t_k), \quad k = 1, 2, \dots, N.$$

Then we derive direct L1 scheme as follows:

$$\partial_t^\alpha u(t_n) = \sum_{k=1}^n c_{n,k}(u(t_k) - u(t_{k-1})) + \bar{r}^n, \quad n = 1, 2, \dots, N,$$

where $c_{n,k}$ and \bar{r}_n are respectively given by

$$c_{n,k} = \frac{(t_n - t_{k-1})^{1-\alpha} - (t_n - t_k)^{1-\alpha}}{\Delta t \Gamma(2-\alpha)}, \quad \bar{r}_n = \frac{1}{\Gamma(1-\alpha)} \sum_{k=1}^n \int_{t_{k-1}}^{t_k} (t_n - \zeta)^{-\alpha} R'_k(\zeta) d\zeta, \quad n = 1, 2, \dots, N.$$

Now, we shall conclude a result as follows.

Proposition 5.1. *Let $m = 0, 1$, and $0 \leq \delta \leq 1$. For $u(t) \in C^{m,\delta}([0, T])$, we have*

$$\max_{1 \leq n \leq N} |\bar{r}_n| \leq C_m \Delta t^{m+\delta-\alpha} \|u\|_{C^{m,\delta}([0, T])},$$

where if $m = 0$, then $\delta \in (\alpha, 1]$ and $C_0 = \frac{\alpha}{\Gamma(1-\alpha)} \left(\frac{2}{\alpha} + \frac{1}{\delta-\alpha} + \frac{1}{1-\alpha} \right)$; and if $m = 1$, then $\delta \in [0, 1]$ and $C_1 = \frac{1}{\Gamma(2-\alpha)}$. In addition, $C^{m,\delta}([0, T])$ denotes Hölder continuous function space equipped with norm

$$\|u\|_{C^{m,\delta}([0, T])} = \sum_{i=0}^m \|\partial_t^i u\|_{C([0, T])} + \sup_{t_1, t_2 \in (0, T); t_1 \neq t_2} \frac{|\partial_t^m u(t_1) - \partial_t^m u(t_2)|}{|t_1 - t_2|^\delta}, \quad 0 \leq \delta \leq 1.$$

Proof. For $m = 1$, the limited smoothness result has been proved in [53, Theorem 2.1] and it can be noted that the solution $u(t)$ has at least the C^1 regularity in time. Next, we consider weak smooth case $m = 0$. Using the following relation

$$R_k(\zeta) = (\zeta - t_k) (u[t_k, \zeta] - u[t_{k-1}, t_k]), \quad \zeta \in (t_{k-1}, t_k), \quad R_k(t_{k-1}) = R_k(t_k) = 0,$$

and integration by parts, we have

$$|\bar{r}_n| = \frac{1}{\Gamma(1-\alpha)} \left| \sum_{k=1}^{n-1} -\alpha \int_{t_{k-1}}^{t_k} (t_n - \zeta)^{-\alpha-1} R_k(\zeta) d\zeta + \int_{t_{n-1}}^{t_n} (t_n - \zeta)^{-\alpha} R'_n(\zeta) d\zeta \right|.$$

Now we shall use integration by parts again to obtain

$$\int_{t_{n-1}}^{t_n} (t_n - \zeta)^{-\alpha} R'_n(\zeta) d\zeta = -\alpha \int_{t_{n-1}}^{t_n} (t_n - \zeta)^{-\alpha-1} R_n(\zeta) d\zeta.$$

Hence, we can bound

$$|\bar{r}_n| \leq \frac{\alpha}{\Gamma(1-\alpha)} \left(\sum_{k=1}^{n-1} \int_{t_{k-1}}^{t_k} (t_n - \zeta)^{-\alpha-1} |R_k(\zeta)| d\zeta + \int_{t_{n-1}}^{t_n} (t_n - \zeta)^{-\alpha-1} |R_n(\zeta)| d\zeta \right).$$

A direct triangle inequality and the definition of Hölder norm in $C^{0,\delta}([0, T])$ space give

$$\begin{aligned} |R_k(\zeta)| &= |(\zeta - t_k) (u[t_k, \zeta] - u[t_{k-1}, t_k])| \leq (t_k - \zeta) (|u[t_k, \zeta]| + |u[t_{k-1}, t_k]|) \\ &= (t_k - \zeta) \left(\left| \frac{u(\zeta) - u(t_k)}{\zeta - t_k} \right| + \left| \frac{u(t_k) - u(t_{k-1})}{t_k - t_{k-1}} \right| \right) \\ &\leq \left((t_k - \zeta)^\delta + \Delta t^{\delta-1} (t_k - \zeta) \right) \|u\|_{C^{0,\delta}([0, T])}, \quad \zeta \in (t_{k-1}, t_k). \end{aligned}$$

Combining $|\bar{r}_n|$ and $|R_k(\zeta)|$ leads to

$$\begin{aligned} |\bar{r}_n| &\leq \frac{2\Delta t^\delta \alpha}{\Gamma(1-\alpha)} \int_0^{t_{n-1}} (t_n - \zeta)^{-\alpha-1} d\zeta \|u\|_{C^{0,\delta}([0, T])} \\ &\quad + \frac{\alpha}{\Gamma(1-\alpha)} \int_{t_{n-1}}^{t_n} (t_n - \zeta)^{-\alpha-1} \left((t_n - \zeta)^\delta + \Delta t^{\delta-1} (t_n - \zeta) \right) d\zeta \|u\|_{C^{0,\delta}([0, T])} \\ &= \frac{2\Delta t^\delta \alpha}{\Gamma(1-\alpha)} \left(\frac{\Delta t^{-\alpha} - t_n^{-\alpha}}{\alpha} \right) \|u\|_{C^{0,\delta}([0, T])} + \frac{\alpha}{\Gamma(1-\alpha)} \left(\frac{\Delta t^{\delta-\alpha}}{\delta-\alpha} + \Delta t^{\delta-1} \frac{\Delta t^{1-\alpha}}{1-\alpha} \right) \|u\|_{C^{0,\delta}([0, T])} \\ &\leq \frac{\alpha \Delta t^{\delta-\alpha}}{\Gamma(1-\alpha)} \left(\frac{2}{\alpha} + \frac{1}{\delta-\alpha} + \frac{1}{1-\alpha} \right) \|u\|_{C^{0,\delta}([0, T])}, \quad \delta > \alpha. \end{aligned}$$

Hence, we end this proof. \square

We can note from Proposition 5.1 that the solution $u(t)$ requires at least the $C^{0,\alpha+\epsilon}$ regularity with arbitrary small $\epsilon > 0$ in time when $m = 0$. The result is consistent with our normal cognition. However, for properly smooth data f and u_0 , though the solution of time fractional diffusion equation is sufficiently smooth for $t > 0$, it usually exhibits a weakly singular behavior at $t = 0$. For more details, see [50, 51, 53].

References

- [1] J. Klafter and I.M. Sokolov. Anomalous diffusion spreads its wings. *Phys. World*, 18(8):29–32, 2005.
- [2] C. Bucur and E. Valdinoci. *Nonlocal diffusion and applications*. Springer, 2016.
- [3] S.W. Duo, H. Wang, and Y.Z. Zhang. A comparative study on nonlocal diffusion operators related to the fractional Laplacian. *Discrete. Cont. Dyn.-B.*, 24:231–256, 2019.
- [4] Q. Du. *Nonlocal Modeling, Analysis, and Computation*. Society for Industrial and Applied Mathematics, Philadelphia, PA, 2019.
- [5] W.H. Deng, R. Hou, W.L. Wang, and P.B. Xu. *Modeling Anomalous Diffusion: From Statistics to Mathematics*. World Scientific, Singapore, 2020.
- [6] R.M. Song and Z. Vondraček. On the relationship between subordinate killed and killed subordinate processes. *Electron. Commun. Probab.*, 13:325–336, 2008.
- [7] R.M. Song and Z. Vondraček. Potential theory of subordinate killed Brownian motion in a domain. *Probab. Theory Relat. Fields.*, 125:578–592, 2003.
- [8] W.H. Deng, B.Y. Li, W.Y. Tian, and P.W. Zhang. Boundary problems for the fractional and tempered fractional operators. *Multiscale Model. Sim.*, 16(1):125–149, 2018.
- [9] R. Metzler and J. Klafter. The random walk’s guide to anomalous diffusion: a fractional dynamics approach. *Phys. Rep.*, 339(1):1–77, 2000.
- [10] A. Sikorskii M.M. Meerschaert. *Stochastic Models for Fractional Calculus*. De Gruyter, Berlin, Boston, 2012.
- [11] I. Golding and E.C. Cox. Physical nature of bacterial cytoplasm. *Phys. Rev. Lett.*, 96:098102, 2006.
- [12] A.M. Edwards, R. Phillips, and et al. Revisiting Lévy flight search patterns of wandering albatrosses, bumblebees and deer. *Nature*, 449:1044–1048, 2007.
- [13] N.E. Humphries, N. Queiroz, and et al. Environmental context explains Lévy and Brownian movement patterns of marine predators. *Nature*, 465:1066–1069, 2010.
- [14] J.W. Kirchner, X.H. Feng, and C. Neal. Fractal stream chemistry and its implications for contaminant transport in catchments. *Nature*, 403:524–527, 2000.
- [15] L.V. Wolfersdorf. On identification of memory kernels in linear theory of heat conduction. *Math. Method. Appl. Sci.*, 17:919–932, 1994.
- [16] X. Liu and W.H. Deng. Numerical approximation for fractional diffusion equation forced by a tempered fractional Gaussian noise. *J. Sci. Comput.*, 84(21), 2020.
- [17] R.H. Nochetto, E. Otárola, and A.J. Salgado. A PDE approach to space-time fractional parabolic problems. *SIAM J. Numer. Anal.*, 54(2):848–873, 2016.
- [18] R.H. Nochetto, E. Otárola, and A.J. Salgado. A PDE approach to fractional diffusion in general domains: a priori error analysis. *Found. Comput. Math.*, 15(3):733–791, 2014.
- [19] A. Bonito, J.P. Borthagaray, R.H. Nochetto, E. Otárola, and A.J. Salgado. Numerical methods for fractional diffusion. *Comput. Vis. Sci.*, 19:19–46, 2018.
- [20] S. Chen and J. Shen. An efficient and accurate numerical method for the spectral fractional Laplacian equation. *J. Sci. Comput.*, 82(17):1–25, 2020.
- [21] A. Bonito and J.E. Pasciak. Numerical approximation of fractional powers of elliptic operators. *Math. Comput.*, 84(295):2083–2110, 2015.
- [22] A. Bonito, W.Y. Lei, and J.E. Pasciak. Numerical approximation of space-time fractional parabolic equations. *Comput. Meth. Appl. Mat.*, 17(4):679–705, 2017.
- [23] A. Bonito, W.Y. Lei, and J.E. Pasciak. The approximation of parabolic equations involving fractional powers of elliptic operators. *J. Comput. Appl. Math.*, 315:32–48, 2017.
- [24] S. Harizanov, R. Lazarov, S. Margenov P. Marinov, and J. Pasciak. Analysis of numerical methods for spectral fractional elliptic equations based on the best uniform rational approximation. *J. Comput. Phys.*, 408:109285, 2020.
- [25] S. Harizanov, R. Lazarov, S. Margenov, and P. Marinov. *The Best Uniform Rational Approximation: Application to Solving Equations Involving Fractional Powers of Elliptic Operators*. IICT-BAS, 2020.
- [26] S. Harizanov, R. Lazarov, S. Margenov, and P. Marinov. Numerical solution of fractional diffusion-reaction problems based on BURA. *Comput. Math. Appl.*, 80:316–331, 2020.

- [27] M. Ilic, F. Liu, I. Turner, and V. Anh. Numerical approximation of a fractional-in-space diffusion equation, I. *Fract. Calc. Appl. Anal.*, 8(3):323–341, 2005.
- [28] Q.Q. Yang, I. Turner, F.W. Liu, and M. Ilic. Novel numerical methods for solving the time-space fractional diffusion equation in two dimensions. *SIAM J. Sci. Comput.*, 33(3):1159–1180, 2011.
- [29] B.J. Szekeres and F. Izsák. Finite difference approximation of space-fractional diffusion problems: the matrix transformation method. *Comput. Math. Appl.*, 73(2):261–269, 2017.
- [30] S.W. Duo, L.L. Ju, and Y.Z. Zhang. A fast algorithm for solving the space-time fractional diffusion equation. *Comput. Math. Appl.*, 75(6):1929–1941, 2018.
- [31] K. Burrage, N. Hale, and D. Kay. An efficient implicit FEM scheme for fractional-in-space reaction-diffusion equations. *SIAM J. Sci. Comput.*, 34(4):A2145–A2172, 2012.
- [32] G. Maros and F. Izsák. Finite element methods for fractional-order diffusion problems with optimal convergence order. *Comput. Math. Appl.*, 80(10):2105–2114, 2020.
- [33] B.J. Szekeres and F. Izsák. Finite element approximation of fractional order elliptic boundary value problems. *J. Comput. Appl. Math.*, 292:553–561, 2016.
- [34] M.L. Zheng, Z.M. Jin, F.W. Liu, and V. Anh. Matrix transfer technique for anomalous diffusion equation involving fractional Laplacian. *Appl. Numer. Math.*, 172:242–258, 2022.
- [35] J.F. Elliott. The characteristic roots of certain real symmetric matrices. Master’s thesis, The university of Tennessee, 1953.
- [36] R.J. LeVeque. *Finite difference methods for ordinary and partial differential equations: steady-state and time-dependent problems*. Society for Industrial and Applied Mathematics, Philadelphia, 1955.
- [37] R.T. Gregory and D. Carney. *A Collection of Matrices for Testing Computational Algorithms*. Wiley-Interscience, New York, 1969.
- [38] J. Gallier. *Discrete Mathematics*. Springer, New York, 2010.
- [39] E. Noble. *The Rise and Fall of the German Combinatorial Analysis*. Springer, Cham, 2022.
- [40] Alien’s Mathematics. Generalized multinomial theorem. <https://fractional-calculus.com/>, 2022.
- [41] L. Ju, J. Zhang, L. Zhu, and Q. Du. Fast explicit integration factor methods for semilinear parabolic equations. *J. Sci. Comput.*, 62:431–455, 2015.
- [42] L. Zhu, L. Ju, and W.D. Zhao. Fast high-order compact exponential time differencing Runge-Kutta methods for second-order semilinear parabolic equations. *J. Sci. Comput.*, 67:1043–1065, 2016.
- [43] S.D. Jiang, J.W. Zhang, Q. Zhang, and Z.M. Zhang. Fast evaluation of the Caputo fractional derivative and its applications to fractional diffusion equations. *Commun. Comput. Phys.*, 21(3):650–678, 2017.
- [44] Y.G. Yan, Z.Z. Sun, and J.W. Zhang. Fast evaluation of the Caputo fractional derivative and its applications to fractional diffusion equations: a second-order scheme. *Commun. Comput. Phys.*, 22(4):1028–1048, 2017.
- [45] Y.X. Huang, Q.G. Li, R.X. Li, F.H. Zeng, and L. Guo. A unified fast memory-saving time-stepping method for fractional operators and its applications. *Numer. Math. Theor. Meth. Appl.*, 15(3):679–714, 2022.
- [46] Y.X. Huang, F.H. Zeng, and L. Guo. Error estimate of the fast L1 method for time-fractional subdiffusion equations. *Appl. Math. Lett.*, 133:108288, 2022.
- [47] L. N. Trefethen and J. A. C. Weideman. The exponentially convergent trapezoidal rule. *SIAM Rev.*, 56(3):385–458, 2014.
- [48] L. Guo, F.H. Zeng, I. Turner, K. Burrage, and G.E. Karniadakis. Efficient multistep methods for tempered fractional calculus: Algorithms and simulations. *SIAM J. Sci. Comput.*, 41(4):A2510–A2535, 2019.
- [49] I. Podlubny. *Fractional Differential Equations*. Academic Press, San Diego, 1999.
- [50] H. Chen and M. Stynes. Blow-up of error estimates in time-fractional initial-boundary value problems. *IMA J. Numer. Anal.*, 41(2):974–997, 2021.
- [51] M. Stynes, E. O’Riordan, and J.L. Gracia. Error analysis of a finite difference method on graded meshes for a time-fractional diffusion equation. *SIAM J. Numer. Anal.*, 55(2):1057–1079, 2017.
- [52] L.L. Bu, L.Q. Mei, and Y. Hou. Stable second-order schemes for the space-fractional Cahn-Hilliard and Allen-Cahn equations. *Comput. Math. Appl.*, 78:3485–3500, 2019.
- [53] T. Zhang and Y. Sheng. The H^1 -error analysis of the finite element method for solving the fractional diffusion equation. *J. Math. Anal. Appl.*, 493:124540, 2021.